SEISMIC-HAZARDS MAPPING OF THE CENTRAL CACHE VALLEY, UTAH —A DIGITAL PILOT PROJECT

by

James P. McCalpin
GEO-HAZ Consulting, Inc.
1221 Graves Ave.
P.O. Box 1377
Estes Park, Colorado 80517
(970) 586-3217, FAX (970) 577-0041
mccalpin@geohaz.com

and

Barry J. Solomon
Utah Geological Survey
1594 West North Temple, Suite 3110
P.O. Box 146100
Salt Lake City, Utah 84114-6100
(801) 537-3388, FAX (801) 537-3400
nrugs.bsolomon@state.ut.us

Digital map compilation by James A. McBride
Utah Geological Survey

Final Technical Report
National Earthquake Hazards Reduction Program
Award No. 1434-HQ-98-GR-00024
Program Element I: Products for Earthquake Loss Reduction

2001

Research supported by U.S. Geological Survey (USGS), Department of the Interior, under USGS award number 1434-HQ-98-GR-00024. The views and conclusions contained in this document are those of the authors and should not be interpreted as necessarily representing the official policies, either expressed or implied, of the U.S. Government.

CONTENTS

FIGURES

TABLES

PLATES

SEISMIC-HAZARDS MAPPING OF THE CENTRAL CACHE VALLEY, UTAH —A DIGITAL PILOT PROJECT

by

James P. McCalpin
GEO-HAZ Consulting, Inc.

and

Barry J. Solomon
Utah Geological Survey

Digital map compilation by James A. McBride
Utah Geological Survey

ABSTRACT

Although the size, timing, and location of future earthquakes are difficult to predict, variations in soil behavior and damage during earthquakes are also controlled largely by mappable geologic and geotechnical site conditions. We evaluate these conditions for the central Cache Valley, Utah, an area undergoing rapid development near the seismically active northern Wasatch Front, using a Geographic Information System. To assess seismic hazards, we analyzed data from geologic maps and a subsurface database compiled from 182 geotechnical boreholes and 1,032 water wells in a study area of 560 kilometers^2. Mapped hazards, at a scale of 1:24,000, include amplified earthquake ground motion, surface fault rupture, liquefaction, and earthquake-induced slope failure. Our procedure for mapping seismic hazards is independent of local geology and may be used elsewhere to assess regional seismic hazards.

We map amplified earthquake ground-motion hazards by delineating near-surface (upper 30 meters) site-response characteristics consistent with Uniform Building Code (UBC), 2000 International Building Code (IBC), and U.S. National Earthquake Hazards Reduction Program (NEHRP) soil-profile types and site classes. We then apply predicted earthquake ground motions to each soil-profile type and modify these predicted earthquake ground motions with amplification factors as outlined in the IBC and NEHRP provisions. Amplification factors as great as 2.8 are associated with long-period (1 second) ground motions in soft clays of soil-profile type S_E. The clays were deposited near the center of the valley by late Pleistocene Lake Bonneville. We map surface-fault-rupture hazards on the valley margins, where the most recent surface-rupturing events occurred from about 4,000 to 4,800 years ago on the West Cache and East Cache fault zones. Special-study areas, extending 150 meters from mapped fault traces on the downthrown side and 75 meters on the upthrown side, are defined where site-specific studies should be performed prior to development. We map liquefaction hazards by assessing subsurface soil conditions, assigning numerical values to the conditions, and designating hazard ratings using summed subsurface values and surficial geologic

characteristics. The liquefaction hazard is high in active flood plains incised into Bonneville clays. We map earthquake-induced slope-failure hazards using published empirical relationships for lateral spreading (soil slopes less than 6 percent), translational landsliding (Newmark displacement of soil slopes greater than 6 percent), and bedrock slope failures. Slope failures are most likely in late Pleistocene to middle Holocene alluvial-levee deposits, latest Pleistocene Lake Bonneville nearshore and deltaic deposits, and Holocene flood-plain alluvium (lateral spreading); soft Tertiary rocks on steep slopes (bedrock slope failures); and existing landslides (translational and bedrock slope failures). Because our hazard maps are intended for use in regional planning and do not reflect site-scale variations in geologic conditions, site-specific geotechnical evaluations are required prior to new construction or upgrading of buildings and other facilities.

INTRODUCTION

Large-scale maps of seismic hazards are valuable tools for land-use planners, engineers, and local government officials. The state of California embarked upon a program to map seismic hazards on 7.5-minute quadrangles, prompted by damaging earthquakes in northern and southern California that resulted in passage by the state legislature of the Seismic Hazards Mapping Act in 1990 (California Division of Mines and Geology, 1997). Other recent examples of large-scale seismic-hazard mapping projects include those undertaken by the Oregon Department of Mineral Industries (Mabey and others, 1993) and the British Columbia Ministry of Energy and Mines (Monahan and others, 2000). In Utah, no comprehensive program to map regional seismic hazards has been completed, although notable studies of individual seismic hazards include 1:48,000-scale maps of liquefaction potential in central and northern Utah (Anderson and others, 1982; 1986a, b; 1990a, b), studies of the potential consequences of tectonic deformation along the Wasatch fault (Keaton, 1986; Chang and Smith, 1998), 1:48,000-scale maps of seismic slope stability along the central Wasatch Front (Keaton and others, 1987), 1:24,000-scale surface-fault-rupture-hazard maps for Wasatch Front counties (Christenson, 1993), and a 1:50,000-scale seismic site-response map of the Salt Lake Valley (Ashland and Rollins, 1999).

Seismic-hazard mapping is most effective for earthquake-hazard reduction when conducted prior to development. Cache Valley, at the northern end of the populous Wasatch Front, is largely rural but experiencing rapid growth as population expands from urban areas (figure 1). The valley contains the tenth largest city in Utah, Logan, as well as numerous smaller communities. Three active fault zones nearby (the Wasatch, West Cache, and East Cache fault zones) pose a significant threat to the region, which was the site of the most damaging earthquake in Utah's history. A magnitude (M_L) 5.7 earthquake occurred on August 30, 1962, near Richmond, about 20 kilometers north of Logan. Over three-fourths of the houses in Richmond were damaged and landslides and rock falls blocked highways and canals. Several large buildings in Logan and Richmond suffered structural damage, and the total estimated earthquake loss was about $1 million (1962 dollars; Lander and Cloud, 1964). Recognizing the seismic risk and history of the region, Green (1977) studied public facilities in Cache Valley to assess their exposure to geologic, including seismic, hazards but did not map hazard potential or susceptibility. We map seismic hazards for four 7.5-minute quadrangles (Newton, Smithfield, Wellsville, and Logan) in central Cache Valley that

Figure 1. *Location map showing four 7.5-minute quadrangles within study area.*

encompass the valley's largest cities and areas that will most likely be developed. Mapped seismic hazards include amplified earthquake ground motion, surface fault rupture, liquefaction, and earthquake-induced slope failure.

Our seismic-hazard maps are intended for both technical and non-technical use. Planners and other local-government officials may incorporate our maps into a land-use plan or local ordinance, adopting requirements similar to our recommendations presented on the maps for site-specific investigations of mapped potential hazards. Geologists and engineers may use technical information on the maps to devise plans for addressing the hazards. Our hazard maps are formatted to stand alone as self-contained products, but may be supplemented by more detailed discussions in the accompanying report.

Although a primary purpose of our study is to map seismic hazards in a specific area, our study also serves as a pilot project to test Geographic Information Systems (GIS) mapping techniques for use elsewhere in Utah. We examine the extent that existing technology can be applied to regional hazard assessment and discuss the limitations of our approach. Our procedures may be adapted to local geology, use existing data sources, and are particularly well suited for use in western Utah's basins. These basins are typically filled with unconsolidated deposits to depths exceeding 30 meters and include large areas of rural land use where geotechnical data are limited.

Our seismic-hazard mapping relies upon both surficial and subsurface data to account for lateral and vertical variations in geotechnical properties. However, surficial Quaternary geologic units in central Cache Valley are commonly thin and overlie deposits with properties that may vary significantly from the general characteristics of surficial units. We therefore map hazard zones employing two techniques: (1) where subsurface data indicate significant shallow variations in stratigraphy we interpolate values between data points to map hazard zones independent of surficial-geologic-unit boundaries, and (2) where subsurface data are lacking, do not vary significantly, or will not significantly affect the hazard potential, we map hazard zones coincident with geologic-unit boundaries. Interpolation is used primarily where deposits of latest Pleistocene Lake Bonneville lie at the surface of the valley floor and are underlain by late Pleistocene deposits of the Little Valley lake cycle and interpluvial alluvium (Scott and others, 1983). Geologic-unit boundaries are used primarily in areas underlain by Holocene alluvium and pre-Quaternary bedrock. Exceptions are noted in sections of this report discussing specific seismic hazards. To account for uncertainties resulting from the irregular distribution of geotechnical data, which is concentrated in areas with preexisting development, we base our division of hazard zones on conservative values of geotechnical parameters. Mabey and others (1993) discuss this issue with regard to a specific hazard (liquefaction), but their comments apply to all hazards: "The consequence of such conservatism is that the mapped hazards...are generally greater than those which would most likely occur during an actual earthquake...This conservatism is desirable in most instances in that it is generally better to overestimate the hazard, which may lead to an unknown excess in the degree of safety, than to underestimate the hazard, which could lead to a false sense of security." Because of this inherent conservatism, our hazard maps are intended primarily for regional planning purposes and should not be used as a substitute for site-specific geotechnical investigations conducted by qualified professionals to more accurately assess hazards.

DATA SOURCES

Geologic Database

The West Cache and East Cache fault zones bound, respectively, the western and eastern edges of the central Cache Valley. Under the National Earthquake Hazards Reduction Program (NEHRP), the U.S. Geological Survey and its contractors produced 1:50,000-scale surficial geologic maps of these fault zones. The Newton and Wellsville 7.5-minute quadrangles were mapped with the West Cache fault zone (Solomon, 1999) and the Logan and Smithfield 7.5-minute quadrangles were mapped with the East Cache fault zone (McCalpin, 1989). The map of McCalpin (1989) was based, in part, on earlier mapping eventually published at a scale of 1:24,000 for the Logan (Evans and others, 1996) and Smithfield (Lowe and Galloway, 1993) quadrangles. Digital versions of Lowe and Galloway (1993), Evans and others (1996), and Solomon (1999) serve as the basis to map hazard zones that are coincident with geologic-unit boundaries and for statistical correlations between subsurface data and surficial geology. We resolved minor differences in geologic interpretations across map boundaries for this study. Because the system for subdivision of Quaternary geologic map units used by Lowe and Galloway (1993) and Evans and others (1996) predated the scheme adopted for the NEHRP maps, we relabeled the Quaternary map units in the Logan and Smithfield quadrangles with their closest equivalent from the NEHRP classification. Of the 70 map units in the four quadrangles, 37 are Quaternary and 33 are pre-Quaternary.

Near-surface geologic conditions that control response to earthquake shaking in the central Cache Valley were dominantly formed by Lake Bonneville in latest Pleistocene time. The lake deposits (the Bonneville Alloformation), which occur at the surface over much of the valley, include a wide variety of grain sizes and depositional environments. Grain size of surficial deposits generally decreases toward the center of the valley as the topographic gradient decreases, with morphologically distinctive nearshore facies of Lake Bonneville (sands and gravels) forming benches on the valley margin, and lake-bottom deposits (silts and clays) underlying much of the central valley floor. Latest Pleistocene to Holocene stream, alluvial-fan, and deltaic deposits are also locally important.

Pre-Quaternary geology is dominated by Precambrian and Paleozoic sedimentary rocks in the Bear River Range on the east side of the valley, in the Wellsville Mountains in the southwest corner of the study area, and on Cache Butte on the northwest edge of the study area. Tertiary rocks are exposed sporadically in the foothills on both valley margins but are most common in the northeast part of the study area. The Precambrian and Paleozoic rocks are commonly much more indurated than the Tertiary rocks, and this property affects amplified earthquake ground-motion and slope-failure hazards.

Geotechnical-Borehole Database

Our principal source of geotechnical-borehole data in the central Cache Valley comes from a comprehensive, unpublished compilation of geotechnical-borehole logs used by Anderson and others

(1990a) for liquefaction-potential mapping. This compilation was supplemented by borehole data from the site of a strong-motion accelerograph on the Utah State University campus in Logan (Shannon & Wilson, Inc., and Agbabian Associates, 1980), and by more recent unpublished borehole data from the Utah Department of Transportation, a geotechnical consultant (Simon-Bymaster, Inc., 1998, 1999), and a geotechnical-testing demonstration conducted in Logan for the First National Conference of the American Society of Civil Engineers Geo-Institute (July, 1997). Borehole data commonly includes descriptions of soil layers, including classification with the Unified Soil Classification System (USCS), and standard-penetration-test (SPT) results; less common are shear-wave velocity profiles, cone-penetrometer-test (CPT) data, and field and laboratory geotechnical-test results such as Atterberg limits, grain-size distribution, moisture content, cohesion, and unconfined compresssive strength.

Our geotechnical database consists of information from 182 boreholes, most of them drilled in clusters to investigate subsurface conditions at 62 sites. The sites are mainly concentrated in urban and suburban areas on the east side of the valley. The boreholes are found in 9 of the 37 Quaternary map units and intersect 1,212 stratigraphic layers. However, most boreholes (140 out of 182) are less than 15 meters deep, the interval we analyze to map liquefaction hazards, and very few (8 out of 182) are as deep as 30 meters, the interval we analyze to map amplified ground motion. Figure 2 shows the distribution of borehole depths and table 1 summarizes characteristics of our geotechnical-borehole database. Plates 1 and 2 show the location of all boreholes, as well as the location of 84 shallow test pits generally less than 3-meters deep. Data from the test pits were not used in our analyses, but may be of use in future site-specific investigations.

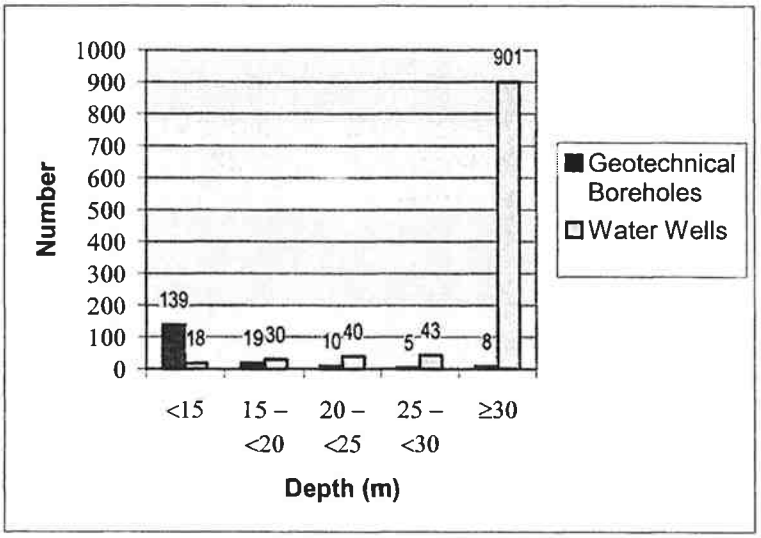

Figure 2. *Histogram showing distribution of borehole and well depths. Data are needed to a depth of 30 meters for analysis of amplified ground motion and to 15 meters for analysis of liquefaction potential.*

Table 1. *Characteristics of the geotechnical-borehole and water-well databases.*

Category	Description	Boreholes	Wells
Distribution	Total	182	1,032
	Total sites	62	1,032
Geology	Quaternary map units drilled	9	22
	Percent of total Quaternary map units	24%	59%
	Total stratigraphic layers intersected by boreholes	1,212	not applicable
Depth	At least 15 meters deep	42	1,014
	Percent at least 15 meters deep	23%	98%
	At least 30 meters deep	8	901
	Percent at least 30 meters deep	4%	87%
Testing	Boreholes with standard penetration test results	182	not applicable
	Percent with standard penetration test results	100%	not applicable
	Boreholes with shear-wave velocity profiles	2	not applicable
	Percent with shear-wave velocity profiles	1%	not applicable
	Boreholes with undrained shear-strength test results	0	not applicable
	Percent with undrained shear-strength test results	0%	not applicable

Water-Well Database

Our sources of data from water wells in the central Cache Valley are reports of well drillers submitted to the Utah Department of Natural Resources, Division of Water Rights. These reports include descriptions of soil layers, but do not include USCS classifications or geotechnical-test results. In contrast to the limited depth and irregular spatial distribution of geotechnical boreholes, water wells in the central Cache Valley are typically deeper than 30 meters and are widely and uniformly distributed. Of 1,032 water wells found in 22 of the 37 Quaternary map units, 1,014 (98 per cent) are deeper than 15 meters and 901 (87 per cent) are deeper than 30 meters. Figure 2 shows the distribution of water-well depths, table 1 summarizes characteristics of our water-well database, and plates 1 and 2 show the location of all water wells.

GEOGRAPHIC INFORMATION SYSTEMS APPROACH

Our maps were produced using ArcView version 3.2 and ArcView Spatial Analyst version 2.0a GIS software (Environmental Systems Research Institute, Inc., 1999, 2000) and are accompanied by a GIS attribute file containing our geologic, geotechnical-borehole, and water-well databases for the central Cache Valley. The creation of the GIS maps and databases allows new data to be readily incorporated and facilitates sharing of existing information which is currently spread among a variety of sources.

AMPLIFIED EARTHQUAKE GROUND-MOTION HAZARDS

Amplification of earthquake ground motion refers to the increase in the intensity of ground

shaking than can occur due to local geological conditions. Amplified ground motion is one of the most serious causes of earthquake damage. The 1962 Cache Valley earthquake (M_L 5.7) caused considerable damage despite relatively modest ground shaking, and the region has the potential for earthquakes much larger than have occurred in historical times. Holocene paleoearthquake magnitudes are estimated to be as large as M_S 7.1 for the Brigham City segment of the Wasatch fault zone (Personius, 1991), M_W 7.1 for the West Cache fault zone (Black and others, 2000), and M_W 6.9 for the East Cache fault zone (McCalpin, 1994).

Mabey and others (1993) mapped amplified earthquake ground-motion hazards of the Portland quadrangle, Oregon, at a scale of 1:24,000 with the computer program SHAKE (Schnabel and others, 1972). However, SHAKE requires knowledge of subsurface thickness and shear-wave velocities. In our study area, shear-wave velocity has been measured in only two boreholes (Shannon & Wilson, Inc. and Agbabian Associates, 1980; Simon-Bymaster, Inc., 1999) (table 1). We could supplement these measurements with shear-wave velocity data from similar deposits elsewhere on the Wasatch Front (King and others, 1987; Wong and Silva, 1993; Williams and others, 1993; Ashland and Rollins, 1999), but Lake Bonneville deposits may have different properties in Cache Valley than elsewhere. Sediment was transported to the lake in Cache Valley primarily by the Bear River, which drains terrain rich in Cretaceous shales and the Eocene Wasatch Formation. Sediment deposited in the lake to the south, where shear-wave velocity measurements are more common, was transported by the Ogden, Weber, and Provo Rivers and other streams draining Paleozoic terrain of the Wasatch Range. The differing clay mineralogy of Bonneville deposits in the two areas may result in different geotechnical parameters such as shear-wave velocity and density. We therefore characterize Cache Valley deposits using local geologic and geotechnical data.

We map amplified earthquake ground-motion hazards using methods employed in the 2000 International Building Code (IBC) (International Code Council, 1997) and U.S. National Earthquake Hazards Reduction Program (NEHRP) provisions (Building Seismic Safety Council, 1997). We first mapped 1997 Uniform Building Code (UBC) soil-profile types (International Conference of Building Officials [ICBO], 1997), which correspond to site classes in the IBC and NEHRP provisions. We then applied predicted earthquake ground motions with a 2 percent probability of exceedance in 50 years (Frankel and others, 1996) to the map of soil-profile types to compute site-amplification factors for appropriate spectral accelerations. These ground motions are recommended by NEHRP in section 4.1.3.1 (Building Seismic Safety Council, 1997) as the maximum considered earthquake ground motions for site-specific investigations. This results in maps of the amplified earthquake ground-motion hazard on which amplification factors for short-period (0.2 second; typically affecting short buildings) and long-period (1 second; typically affecting tall buildings) motions are related to the mapped limits of UBC soil-profile types (plates 1A through 1D).

Mapping Procedure

The UBC defines six soil-profile types, designated S_A through S_F, by shear-wave velocity, standard penetration test (SPT) results, or undrained shear strength in the upper 30 meters of soil (table 2). Because shear-wave-velocity measurements are rare in our study area, and undrained-shear-strength measurements are absent (table 1), we rely upon SPT data. These data were measured

in 182 geotechnical boreholes, but only eight of the boreholes were drilled to depths of at least 30 meters. In contrast to the limited depth and irregular spatial distribution of geotechnical boreholes, water wells in the central Cache Valley are typically deeper than 30 meters and are widely and uniformly distributed. Of 1,032 water wells in the area, 901 are at least 30 meters deep. Therefore, we use water-well logs to determine subsurface stratigraphy of the upper 30 meters of soil and geotechnical-borehole logs to determine the relationship between SPT data and subsurface stratigraphy. We then estimate SPT values for stratigraphic units in water wells by correlation with Unified Soil Classification System (USCS) classes in geotechnical boreholes. This link between abundant water-well logs and the correlation between SPT data and subsurface stratigraphy in geotechnical boreholes, supplemented by surficial-geologic map data, enable us to map soil-profile types. Because geologic interpretations based on water-well logs are less precise than interpretations of borehole logs, the use of water-well logs is appropriate only for regional studies in areas where geotechnical data are sparse or lacking. Water-well logs should not be relied upon for site-specific investigations.

Table 2. *Criteria to define UBC soil-profile types.*

Soil-Profile Type	Shear-Wave Velocity[1] v_s (m/s)	Standard Penetration Test[1] N (blows/ft)	Undrained Shear Strength[1] s_u (kPa)
S_A	>1,500	n.a.	n.a.
S_B	760-1,500	n.a.	n.a.
S_C	360-760	>50	>100
S_D	180-360	15-50	50-100
S_E[2]	<180	<15	<50
S_F	Soil requiring site-specific evaluations		

[1] v_s, N, and s_u refer to average values in the upper 30 meters of soil or rock.
[2] Soil-profile type S_E also includes any soil profile with more than 3 meters of soft clay, defined as soil with plasticity index>20, moisture content≥40%, and s_u<25kPa.
n.a.-not applicable.

To map the soil-profile types, we follow the UBC method (ICBO, 1997) for classifying a single site. That method begins with identifying small areas of soil with the worst conditions (soil-profile types S_E and S_F), then considers the remaining soil conditions (soil-profile types S_C and S_D), and finally considers bedrock (soil-profile types S_A and S_B) where ground-motion amplification is, by definition, the smallest. Although our procedure for mapping soil-profile types uses SPT data, it may be adapted for use in other areas where shear-wave velocity or undrained shear strength data are more abundant. Refer to the UBC (p. 2-23 through 2-24) for guidance using shear-wave velocity or undrained shear strength.

Map Soil-Profile Type S_F (Soil Requiring Site-Specific Evaluation)

Step 1: Identify soils vulnerable to potential failure or collapse under seismic loading such as liquefiable soils, quick and highly sensitive clays, and collapsible weakly cemented soils.

a. Liquefiable soils—the procedure for mapping liquefiable soils is outlined in the section of this report on liquefaction hazards.
b. Quick and highly sensitive clays—Identify any borehole logs that contain USCS classes

CL and CH (inorganic clays) with sensitivities (the ratio of unconfined compressive strength before and after remolding) greater than 30 in the upper 30 meters of soil. If present, draw a boundary around the boreholes from which the geotechnical data were obtained to define an area of soil-profile type S_F.

c. Collapsible weakly cemented soils—Identify any borehole logs that contain soils with low unit weight, high void ratios, weak cementation, and evidence of collapse when saturated in consolidation tests in the upper 30 meters of soil. If present, draw a boundary around the boreholes from which the geotechnical data were obtained to define an area of soil-profile type S_F.

Step 2: Identify peats and highly organic clays.

a. Identify any borehole logs that contain USCS classes PT (peat), OH (organic clay), or OL (organic silty clay) with a cumulative thickness greater than 3 meters in the upper 30 meters of soil.
b. If the soils identified in step 2.a. can be correlated with a surficial-geologic map unit, and the unit is generally greater than 3 meters thick, define the entire map unit as an area of soil-profile type S_F.
c. If the soils identified in step 2.a. cannot be correlated with a surficial-geologic map unit, or the unit is generally less than 3 meters thick, draw a boundary around the boreholes where the soils were identified to define an area of soil-profile type S_F.

Step 3: Identify very high plasticity clays.

a. Identify any borehole logs that contain USCS class CH (inorganic clay) with a plastic index greater than 75 and a cumulative thickness greater than 8 meters in the upper 30 meters of soil. If present, draw a boundary around the boreholes from which the geotechnical data were obtained to define an area of soil-profile type S_F.

Step 4: Identify very thick soft/medium-stiff clays.

a. Identify any borehole logs that contain USCS classes CL and CH (inorganic clays) with an unconfined compressive strength less than 25 kilopascals, water content greater than (or equal to) 40 per cent, plastic index greater than 20, and a cumulative thickness greater than 36 meters. If present, draw a boundary around the boreholes from which the geotechnical data were obtained to define an area of soil-profile type S_F.

Step 5: Save the map on which soils with soil-profile type S_F are identified as map layer 1.

Map Soft Clay Within Soil-Profile Type S_E (Soft Soil)

Step 1: Identify soft clays.

a. Identify any borehole logs that contain USCS classes CL and CH (inorganic clays) with an unconfined compressive strength less than 25 kilopascals, water content greater than (or equal to) 40 per cent, plastic index greater than 20, and a cumulative thickness greater than 3 meters but less than 36 meters. If present, draw a boundary around the boreholes from which the geotechnical data were obtained to define an area of soil-profile type S_E.

Step 2: Save the map on which soft clays within soil-profile type S_E are identified as map layer 2.

Map Soil-Profile Types S_C, S_D, and the Remainder of S_E (Very Dense, Stiff, and Soft Soil)

Step 1: Compute the average field SPT value (N in blows/foot) for each distinctly different soil layer shallower than 30 meters for which SPT data were collected in geotechnical boreholes. The term "distinctly different soil layer" is specified, but not defined, in the UBC (ICBO, 1997, p. 2-24). We define such a soil layer as one including all contiguous soil within an individual USCS class, regardless of thickness, as opposed to a single layer whose thickness is defined by the testing interval.

a. Compute N for each layer shallower than 30 meters in which SPT data were measured in boreholes at least 30 meters deep and for each layer in which SPT data were measured in boreholes less than 30 meters deep. N for boreholes less than 30 meters deep will not be used to map soil-profile types but will be used to establish the correlation between N and USCS classes.
b. If the testing intervals for all SPTs within a layer are equal, N is the average value of all SPTs within the layer; if the testing intervals are unequal, N is the weighted average value.

Step 2: Assign a value for N to each distinctly different soil layer shallower than 30 meters for which SPT data were not collected in geotechnical boreholes at least 30 meters deep.

a. Assign a value for N based on the nearest measured N in a layer of the same USCS class within the same borehole.
b. If N has not been measured in a layer of the same USCS class within the same borehole, use a measured value from a layer with the same USCS class at approximately the same depth in the nearest borehole.

Step 3: Establish a correlation between N and average layer depth for each USCS class and resistant strata found in geotechnical boreholes by computing a least-squares regression using data from step 1 (measured values); do not use data from step 2 (assigned values). Correlations for the central Cache Valley are shown in table 3.

Step 4: Create an equivalence table listing all soil types in water-well logs and their most likely equivalent USCS class. Establishing equivalence is primarily based on the description of material on driller's logs, but may be modified because of the lack of detail in the description. Modifications may be based on additional driller's remarks recorded on the logs regarding soil properties and on the relationship between local depositional environments and the expected sorting and mechanical properties of Quaternary sediments. Soil types recorded on water-well logs from the central Cache Valley and their equivalent USCS classes are shown in table 4.

Step 5: If geotechnical boreholes and water wells are near each other, check the accuracy of the

Table 3. *Correlations between N and depth for USCS classes encountered in geotechnical boreholes and resistant strata encountered in water wells from the central Cache Valley.*

USCS Class or Resistant Strata Lithology	Number of Samples	Average Measured N (blows/ft)	Correlation between N and Depth (D) in feet	Depth Dependence of N	Comments
CL	112	10.6	11.7 + 0.01D	Weak	Clay is relatively incompressible
ML	118	18.2	16.0 + 0.07D		
SC	10	7.8	5.9 + 0.08D		
SM	56	25.0	16.7 + 0.23D	Strong	Sand readily compresses
SM/ML	7	24.6	14.0 + 0.23D		
SP	12	26.5	17.1 + 0.39D		
SW	5	32.4	21.1 + 0.30D		
GC	3	29.0	12.4 + 0.61D		Poorly sorted gravels, most with fine-grained matrix, readily compress
GM	95	55.6	48.9 + 0.24D		
GW	47	59.6	50.3 + 0.45D		
GP	35	54.7	57.5	None	Well-sorted gravels with no fine-grained matrix are relatively incompressible
Conglomerate	Value for N is estimated		75		Consolidated material is relatively incompressible
Hardpan			75		
Bedrock			100		

Table 4. *Soil types in water-well logs and their equivalent USCS classes, central Cache Valley, Utah.*

Soil Type						USCS Class	Comments
Clay	Silt	Sand	Gravel	Cobbles	Other (Topsoil)		
X						CL	All clays in geotechnical boreholes are CL
X	X					ML	All silts in geotechnical boreholes are ML
X		X				SC	We assume sand is more abundant than clay because sandy clays are less common in geotechnical boreholes
	X					ML	All silts in geotechnical boreholes are ML
	X	X				SM/ML	We assume sand is more abundant than silt because silty clays are less common in geotechnical boreholes
		X				SW	Most wells with sand are drilled in alluvial fans, where sand is typically poorly sorted
X			X			GC	No intermediate grain sizes noted in logs
	X		X			GM	Most wells with gravel are drilled in alluvial fans; alluvial-fan gravels with fine-grained material in boreholes are typically silty
X		X	X			GM	Most wells with gravel are drilled in alluvial fans; alluvial-fan gravels with fine-grained material in boreholes are typically silty
		X	X			GP	We assume gravel is well sorted because of the absence of fine-grained material and the presence of sand
			X			GW	Most wells with gravel are drilled in alluvial fans; alluvial-fan gravels are typically poorly sorted
X				X		GC	No intermediate grain sizes noted in logs
			X	X		GP	We assume gravel is well sorted because of the absence of fine-grained material
				X		GP	We assume gravel is well sorted because of the absence of fine-grained material
					X	ML	Most local topsoil includes wind-blown silt

equivalence table by comparing the logs of the adjacent boreholes and wells. Modify the equivalence table if necessary.

Step 6: Assign an equivalent USCS class from the equivalence table (step 4) to all soil layers in the water-well database.

Step 7: Use the correlations between N and average layer depth for each USCS class and resistant strata (step 3) to compute the equivalent N value for all soil layers in the water-well database.

Step 8: Compute the average N value for the upper 30 meters in each geotechnical borehole and water well at least 30-meters deep using equation 1 (modified from ICBO, 1997, equation 36-2):

Eq. 1 $N_{30} = \sum d_i / \sum (d_i / N_i)$

where:

$\sum$ = sum of the appropriate value for all layers from layer $i = 1$ to n in the upper 30 meters of the soil profile.

N_{30} = average SPT value in the upper 30 meters of the soil profile, in blows per foot.

d_i = thickness of layer i, in feet.

N_i = SPT value of layer i either in accordance with approved nationally recognized standards (for geotechnical boreholes) or equivalent values (for water wells), in blows per foot.

Step 9: Interpolate a grid of regularly spaced N_{30} values from the irregularly spaced borehole and well data. Parameters for interpolation may vary depending upon the characteristics of data within a particular study area. For the central Cache Valley, we use a cell size of 80 meters and an Inverse Distance Weighting algorithm. The value for N_{30} at each grid cell was computed based on the weighted average of all values within a 2,000-meter radius of the grid cell, using a distance-weighting exponent of –2 (the values were therefore multiplied by the inverse of the square of their distance from the grid cell). The 80-meter cell size is the largest cell size possible without placing more than one value within a grid cell. The 2,000-meter radius is the smallest radius possible that eliminates most isolated areas created by the effect of an anomalous value. The distance-weighting exponent of –2 reduces the influence of distant wells compared to an exponent of –1.

Step 10: Contour N_{30} for all geotechnical boreholes and water wells at least 30 meters deep at values of 15 and 50. The map defines areas of soil-profile types S_C ($N_{30} > 50$) and S_D ($N_{30} = 15$ to 50) and any areas of S_E ($N_{30} < 15$) not previously identified by the presence of soft clays (table 2).

Step 11: Within each of the major areas of soil-profile types, remove small, isolated areas of anomalous soil-profile types because their inclusion represents a level of detail not supported by the inherent uncertainties of water-well data.

Step 12: Modify the contour map to reflect surficial geology in areas where bedrock is shallow and subsurface data are not available. In the central Cache Valley, subsurface data are not available from colluvium and alluvium in mountain canyons and on shallow bedrock along the Bear River Range front. The closest subsurface data results in classification of these areas as soil-profile types S_D or S_E, but the coarse grain size of this material indicates that the geologic-map units should be assigned to soil-profile type S_C.

Step 13: Save the map on which soils with soil-profile types S_C, S_D, and S_E (not previously identified by the presence of soft clays) are identified as map layer 3.

Map Soil-Profile Types S_A and S_B (Hard Rock and Rock)

Step 1: Differentiate soil-profile types S_A (hard rock) and S_B (rock).

a. If shear-wave-velocity measurements are available, assign geologic-map units with shear-wave velocities greater than 1,500 meters/second to soil-profile type S_A and geologic-map units with shear-wave velocities between 760 and 1,500 meters/second to soil-profile type S_B (table 2).
b. If shear-wave-velocity measurements are not available, assign geologic-map units to soil-profile types S_A or S_B based on the degree of induration. Assign geologic-map units composed primarily of hard, compact, well-cemented rock to soil-profile type S_A and geologic-map units composed primarily of softer, weakly cemented rock to soil-profile type S_B.

Step 2: Save the map on which rock with soil-profile types S_A and S_B are identified as map layer 4.

Compile Map Layers

Overlay map layers 1 through 4 in the following order to produce a composite map of soil-profile types. This procedure ensures identification of small areas of soil-profile types S_E and S_F within broader areas of other soil-profile types. If the procedure is reversed, broad areas will cover and replace smaller areas.

Step 1: Combine map layers 3 (soil-profile types S_C, S_D, and the remainder of S_E) and 4 (soil-profile types S_A and S_B). Because map layer 3 includes soil-profile types only within unconsolidated soil and map layer 4 includes soil-profile types only within bedrock, the areas identified on the layers will not overlap and the order in which the layers are overlain does not matter.

Step 2: Overlay map layers 1 (soil-profile type S_F) and 2 (soft clay within soil-profile type S_E) on the product of step 1. Because map layers 1 and 2 identify unique areas that will not overlap, the order in which layers 1 and 2 are overlain does not matter.

Determine Amplification Factors and Local Accelerations

Step 1: Specify spectral accelerations—The degree to which ground motions are amplified depends on the period of the ground motions and the size of the accelerations. Ground motions with short periods (0.2 seconds) typically affect short buildings; ground motions with long periods (1.0 seconds) typically affect tall buildings. The NEHRP provisions and IBC state that the maximum considered earthquake ground motion for site-specific procedures shall be taken as that motion represented by a 5 percent damped acceleration response spectrum having a 2 percent probability of exceedance within a 50-year period. Determine this acceleration for both short- and long-period ground motions from the regional seismic-hazard maps of Frankel and others (1996). Accelerations for specific geographic coordinates may also be obtained from the U.S. Geological Survey (USGS) on the World Wide Web at http://geohazards.cr.usgs.gov/eqint/html/lookup.shtml. Spectral accelerations at the center of our four-quadrangle study are shown in table 5.

Step 2: Determine amplification factors.

a. NEHRP tabulates amplification factors (referred to as acceleration-based site coefficients, F_a) for short-period spectral accelerations (S_S) in table 4.1.2.4a (Building Seismic Safety Council, 1997) as a function of NEHRP site class (UBC soil-profile type). Use the short-period spectral acceleration determined in step 1 to determine the short-period amplification factors for each soil-profile type. Use straight-line interpolation for intermediate values of S_S not specified in the table. Short-period amplification factors at the center of our four-quadrangle study area are shown in table 5.

b. NEHRP tabulates amplification factors (referred to as velocity-based site coefficients, F_v) for long-period spectral accelerations (S_1) in table 4.1.2.4b (Building Seismic Safety Council, 1997) as a function of NEHRP site class (UBC soil-profile type). Use the long-period spectral acceleration determined in step 1 to determine the long-period amplification factors for each soil-profile type. Use straight-line interpolation for intermediate values of S_1 not specified in the table. Long-period amplification factors at the center of our four-quadrangle study area are shown in table 5.

Step 3: Calculate local accelerations—Calculate local ground accelerations by multiplying spectral accelerations determined in step 1 by amplification factors determined in step 2 for each soil-profile type and ground-motion period.

Results

Using the procedures outlined above, our map of UBC soil-profile types and related amplification factors (plates 1A through 1D) exhibit a pattern that can be readily explained by the geologic history of the central Cache Valley. The distribution of soil-profile types is consistent with both surficial and subsurface geology, reflecting basin geomorphology dominated by late Pleistocene lacustrine and alluvial deposition.

Table 5. *Ground motions and characteristics of UBC soil-profile types in the central Cache Valley, Utah.*

Soil-Profile Type (Site Class)	Ground Motion						Characteristics	
	Short Period (0.2 seconds) (typically affecting short buildings[1])			Long Period (1 second) (typically affecting tall buildings[1])			Standard Penetration Test (blows/ft)[6]	Geology
	Spectral Acceleration (g)[2]	Amplification Factor[3]	Local Acceleration (g)[5]	Spectral Acceleration (g)[2]	Amplification Factor[4]	Local Acceleration (g)[5]		
S_A	1.02	0.8	0.8	0.32	0.8	0.3	n.a.	Hard rock–includes all Paleozoic and Precambrian bedrock units; strongly indurated.
S_B	1.02	1.0	1.0	0.32	1.0	0.3	n.a.	Rock–includes all Tertiary units; weakly indurated.
S_C	1.02	1.0	1.0	0.32	1.5	0.5	>50	Very dense soil–generally coarse-grained deposits with gravel, cobbles, or boulders; includes alluvium and alluvial-fan deposits of major canyons and local areas of shallow bedrock near the range front, but does not necessarily conform to boundaries of geologic units.
S_D	1.02	1.1	1.1	0.32	1.8	0.6	$15 < N < 50$	Stiff soil–includes clays of the Bonneville and Little Valley lake cycles and coarser deposits of interpluvial alluvial fans from major drainages.
S_E	1.02	0.9	0.9	0.32	2.8	0.9	< 15	Soft soil-includes lake clays beyond the distal edges of the pre-Bonneville buried fan gravels.
S_F	Site-specific geotechnical investigation and dynamic site-response analysis shall be performed[7]						Not mapped, but may locally occur.	

1 The critical period of ground motion for a specific building or building type should be determined by a qualified structural engineer.

2 Maximum considered earthquake spectral-response accelerations mapped by Frankel and others (1996) based on acceleration at center of four-quadrangle study area with 2% probability of exceedance in 50 years used in IBC and NEHRP provisions. The UBC uses seismic zone factors based on peak accelerations with a 10% probability of exceedance in 50 years.

3 Acceleration-based site coefficient from NEHRP recommended provisions (Building Seismic Safety Council, 1997, tab. 4.1.2.4a).

4 Velocity-based site coefficient from NEHRP recommended provisions (Building Seismic Safety Council, 1997, tab. 4.1.2.4b).

5 Local Acceleration = Spectral Acceleration x Amplification Factor.

6 Standard Penetration Test (blows/foot) in geotechnical borings or equivalent value predicted for water wells. Range of values for soil-profile types S_C, S_D, and S_E are specified by the Uniform Building Code (International Conference of Building Officials, 1997). n.a.–not applicable.

7 International Conference of Building Officials (1997). Soils requiring site-specific evaluations include soils vulnerable to potential failure or collapse during earthquake ground shaking such as liquefiable soils (shown on plate 2 of this report), quick and highly sensitive clays, and collapsible weakly cemented soils; peats and highly organic clays thicker than 3 meters; very high plasticity clays thicker than 8 meters; and very thick soft/medium stiff clays thicker than 36 meters.

Soil-profile types S_A and S_B are predominant on the valley margins, reflecting bedrock geology. Soil-profile type S_A includes Precambrian and Paleozoic rocks in the Bear River Range on the east side of the valley, in the Wellsville Mountains in the southwest corner of the study area, and on Cache Butte on the northwest edge. Soil-profile type S_B includes Tertiary rocks in mountain foothills, and is particularly common in the northeast corner of the study area (plate 1B), northeast of Hyde Park. We differentiate these soil-profile types based on the degree of induration because shear-wave velocity data are not available. Precambrian and Paleozoic rocks consist primarily of hard quartzite and limestone, whereas Tertiary rocks consist primarily of softer tuff and volcaniclastic sedimentary rock.

Soil-profile type S_C is found in mountain canyons and in small areas along the range front. Deposits included within this soil-profile type are very coarse grained, with common gravel- to boulder-sized clasts. Because subsurface data are rare within these deposits, we define the distribution of the soil-profile type largely by the distribution of characteristic surficial-geologic units. The largest areas of type S_C are defined by surficial geology and consist of upper to middle Pleistocene fan alluvium east of Hyde Park at the base of the Bear River Range (plate 1B) and southwest of Mendon at the base of the Wellsville Mountains (plate 1C). Surficial geology is also the basis for classifying type S_C in mountain canyons of the Bear River Range and Wellsville Mountains, which are underlain by middle Pleistocene to Holocene alluvium and colluvium. The extent of type S_C at the mouths of Smithfield and Green Canyons, respectively near Smithfield and North Logan (plate 1B), is supported by subsurface data.

Soil-profile types S_D and S_E are predominant on the valley floor, but their distribution is closely associated with topography. The topography is related to surficial geology, but subsurface geology largely controls soil properties within depths of 30 meters from the ground surface.

Soil-profile type S_D is found primarily on piedmont slopes. These slopes are more common on the east side of the valley, where major canyons drain the Bear River Range (plates 1B and 1D), and are also found in a narrower band at the base of the Wellsville Mountains to the west (plate 1C) and in the northwest corner of the central Cache Valley (plate 1A) near Little Mountain, which is northwest of the study area. The surficial geology of piedmont slopes is dominated by deposits of latest Pleistocene Lake Bonneville, but interpluvial alluvium underlies Bonneville deposits and overlies deposits of the late Pleistocene Little Valley lake cycle. This alluvium includes significant amounts of sand and gravel, imparting a stiffness to the soil that is absent in softer lacustrine deposits. Thus, the inclusion of most piedmont slopes within soil-profile type S_D results from the properties of subsurface interpluvial alluvium rather than the properties of surficial-geologic units.

Soil-profile type S_E is found primarily on the nearly flat valley bottom in the vicinity of the Little Bear River (plates 1A and 1C). Here, the river is incised into fine-grained sediment deposited by Lake Bonneville. This area is generally beyond the distal part of the interpluvial alluvial fans which underlie piedmont slopes and, because the surficial alluvium is thin, the soil profile in the upper 30 meters is dominated by soft lacustrine clays from both the Bonneville and Little Valley lake cycles. Soil-profile type S_E also is found in the northeast part of our study area, extending eastward in a narrow band from Cutler Reservoir to Hyde Park (plates 1A and 1B). This extension lacks

interpluvial alluvium because, although it lies closer to the Bear River Range front, it occurs between the clastic influence of the Logan River (Logan Canyon) and Summit Creek (Smithfield Canyon). Surficial expression of the lack of significant clastic input by these two major drainages in this area is shown by its low surface gradient and position between convex piedmont slopes extending outward from the canyons.

Amplified earthquake ground-motion hazards in the central Cache Valley reflect variations in the mapped pattern of soil-profile types, but the magnitude of amplification also depends upon spectral accelerations (table 5). For example, amplification factors for long-period (1 second) ground motions range from 0.8 (which results in attenuation, or a decrease, in ground motions) in soil-profile type S_A to 2.8 (significant amplification) in soil-profile type S_E. For long-period ground motions, intermediate soil-profile types are associated with intermediate amplification factors. However, amplification factors for short-period (0.2 seconds) ground motions only increase from 0.8 to 1.1 from soil-profile types S_A to S_D, and then decrease to 0.9 in soil-profile type S_E. The large difference in amplification factors for long-period ground motions suggests the importance of effectively differentiating soil-profile types in site-specific geotechnical investigations. Our recommendations for the need to conduct site-specific investigations are shown in table 6.

Amplification by soft soils (soil-profile type S_E) diminishes as the strength of ground shaking increases (Building Seismic Safety Council, 1997). Consequently, amplification by soft soils may be less and actually attenuate motions during strong ground shaking generated by a nearby large earthquake, but could be significant for moderate ground shaking generated either by a more distant large earthquake or nearby moderate earthquake. However, moderate ground shaking occurs more frequently, so that areas on our maps assigned a high amplification factor will be subjected to potentially damaging ground motion more often than areas assigned a low amplification factor.

Our maps provide a regional assessment of amplified earthquake ground-shaking hazards in the central Cache Valley, but care should be used for proper application of the mapping techniques and data. We use data from water wells because they are more widespread than geotechnical boreholes in our study area. However, geologic interpretations based on water-well logs are less precise than interpretations of borehole logs. The use of water-well logs is appropriate only for regional studies in areas where geotechnical data are sparse or lacking. Water-well logs should not be relied upon for site-specific investigations. We use SPT data for mapping soil-profile types. However, Ashland and Rollins (1999) demonstrate that the interpretation of soil-profile types in the Salt Lake Valley, and perhaps elsewhere, depends upon the method of characterizing near-surface soils. They report that the SPT method tends to classify soils into more conservative soil-profile types (for example, S_E rather than S_D or S_D rather than S_C) than do the shear-strength and shear-wave velocity methods. A conservative interpretation of soil-profile types is reflected in a tendency toward more conservative mapping of amplified ground motion in our regional assessment, which should be addressed in site-specific studies.

Mapped amplified ground-motion hazards reflect variations due to soil conditions, which are applicable to most earthquakes that will affect the region. However, our maps do not address near-fault, topographic, and three-dimensional effects, which are more dependent on the earthquake

Table 6. *Recommended requirements for site-specific investigations of mapped potential hazards.*

Hazard	Soil-Profile Type, Special-Study Area, or Potential-Hazard Area		Development Type			
			Essential Facilities, Special- and High-Occupancy Buildings	Industrial and Commercial Buildings (Other Than High-Occupancy)	Residential Subdivisions	Residential Single Lots
Amplified Ground Motion (Plate 1)	S_A, S_B		No	No	No	No
	S_C, S_D, S_E		Yes	Yes	No	No
	S_F		Yes	Yes	Yes	Yes
Surface Fault Rupture (Plate 1)	Inside Special-Study Area	Holocene Fault	Yes	Yes	Yes	Yes
		Quaternary Fault	Yes	No[1]	No[1]	No[1]
	Outside Special-Study Area		Yes	No	No	No
Liquefaction (Plate 2)	High, Moderate		Yes	Yes	No[2]	No[2]
	Low, Very Low		Yes	No	No	No
	Not Susceptible		No	No	No	No
Slope Failure[3] (Plate 3)	Very High, High, Moderate		Yes	Yes	Yes	Yes
	Low, Very Low		Yes	No	No	No

[1] At a minimum, appropriate disclosure should be required.

[2] At a minimum, appropriate disclosure should be required. If a site is also within an area with high or moderate potential for lateral spreading (earthquake-induced slope failure caused by liquefaction on shallow slopes; see plate 3), a site-specific investigation is advised consistent with recommendations for slope-failure hazards.

[3] If permanent cuts have slopes steeper than 2H:1V (50 percent) and are not supported by retaining walls, cut-slope stability must be addressed in accordance with the Uniform Building Code (International Conference of Building Officials, 1997, Appendix Chapter 33, section 3312).

location and direction of seismic-energy propagation, nor do we consider amplification of ground motion due to resonance. Near-fault effects refer to spatial variations in ground motion amplitude and duration near the fault causing the earthquake that may result in ground motions greater than anticipated at sites near surface traces of active faults (the West Cache and East Cache fault zones). These effects are particularly significant for structures, such as tall buildings, that are sensitive to long-period ground motions (Somerville and others, 1997). Topographic effects refer to amplification of ground motion due to the configuration of the ground surface. Topographic amplification can exceed amplification due to soil conditions in some cases, and is commonly experienced on hills, ridges, and the tops of cliffs (Somerville, 1998). Three-dimensional effects refer to the focusing of energy due to the structure of the earth's crust in the region, which may result in amplification as great as amplification due to soil conditions (Somerville, 1998). Amplification of ground motion due to resonance may occur because the specific periods of earthquake-induced ground motion match the natural periods of a site. This effect can be particularly destructive to structures whose natural periods match those of the site (Rial and others, 1992).

SURFACE-FAULT-RUPTURE HAZARDS

During a large earthquake, fault rupture at depth may propagate upward and displace the ground surface, forming a main scarp and adjacent zone of deformation. The zone of deformation, typically more extensive on the downthrown side of normal faults, includes features such as ground cracks and tilted and downdropped blocks. Surface fault rupture and associated deformation can damage or destroy structures and sever lifelines (pipelines, utilities, and transportation routes).

Faults that show evidence of repeated surface displacement during Quaternary time, and particularly faults with evidence of Holocene displacement, represent potential hazards to development. Two fault zones in the central Cache Valley, the West Cache and East Cache fault zones, show clear evidence of Holocene displacement. The Wellsville fault, part of the West Cache fault zone, bounds the west side of the valley in the Wellsville quadrangle (plate 1C). The most recent surface-faulting event on the Wellsville fault occurred between 4,400 and 4,800 years ago (Black and others, 2000). The Junction Hills fault, also part of the West Cache fault zone, extends into the western margin of the Newton quadrangle (plate 1A). The most recent surface-faulting event on the Junction Hills fault occurred between 8,250 and 8,650 years ago (Black and others, 2000). The central segment of the East Cache fault zone bounds the east side of the valley in the Logan and southern Smithfield quadrangles (plates 1B and 1D). The most recent surface-faulting event on this segment occurred about 4,000 years ago (McCalpin, 1994). The northern and southern segments of the East Cache fault zone bound the east side of the valley, respectively, in the northern Smithfield quadrangle (plate 1B) and on the southern edge of the Logan quadrangle (plate 1D). Although the northern and southern segments show evidence of Quaternary displacement, the most recent surface faulting occurred on the northern segment at least 15,000 years ago and on the southern segment between about 26,000 and 46,000 years ago (McCalpin, 1994).

We map the surface-fault-rupture hazard by showing main fault traces with a significant potential for future movement in the central Cache Valley and their associated special-study areas

(plates 1A through 1D). Fault traces are compiled from existing geologic maps (Lowe and Galloway, 1993; Evans and others, 1996; Solomon, 1999) and are differentiated into two groups by the age of most recent surface displacement: Holocene faults are distinguished from faults on which the most recent surface displacement is Quaternary but pre-Holocene. Special-study areas bound the fault traces, extending 150 meters from faults on the downthrown side and 75 meters on the upthrown side. Site-specific investigations addressing surface-fault-rupture hazards are recommended in special-study areas because the fault maps are not detailed enough to include all fault traces and delineate zones of deformation at a particular location. Studies should be performed prior to development to evaluate earthquake history, characterize the zone of deformation, and determine fault setbacks. Our recommended requirements for site-specific investigations are shown on table 6.

LIQUEFACTION HAZARDS

Liquefaction occurs during earthquakes when shallow, water-saturated, cohesionless soils are subjected to ground shaking. Upon liquefaction, susceptible soils lose their strength and ability to support the weight of overlying sediments and structures. Liquefaction is one of the major causes of earthquake damage. During the 1962 Cache Valley earthquake (M_L 5.7), liquefaction occurred along the banks of the Bear River near Trenton (about 25 kilometers northwest of Logan) when liquefied sand was extruded from cracks and sand boils (Hill, 1979).

The Southern California Earthquake Center (SCEC, 1999) proposed procedures for mapping liquefaction hazards to implement the Seismic Hazards Mapping Act in California. According to the SCEC, liquefaction hazard zones meet one or more of the following criteria:

1. Areas where liquefaction has occurred during historical earthquakes.
2. Areas of uncompacted or poorly compacted fills containing liquefaction-susceptible materials that are saturated, nearly saturated, or may be expected to become saturated.
3. Areas where sufficient existing geotechnical data and analyses indicate that the soils are potentially susceptible to liquefaction.
4. Areas where geotechnical data are lacking or insufficient, with susceptibility identified by the age of unconsolidated material, depth to ground water, and peak ground acceleration.

Mabey and others (1993) mapped liquefaction susceptibility of the Portland, Oregon 7.5-minute quadrangle. Because geotechnical data and analyses were available, the quadrangle was mapped using SCEC criterion 3. Mabey and others (1993) used the procedure of Youd (1991) to map liquefaction susceptibility, which incorporates techniques discussed by Seed and others (1983, 1985) for evaluation of liquefaction potential using field-performance data.

Because geotechnical data in the central Cache Valley are sparse, liquefaction potential must be mapped by applying the fourth SCEC criterion, using the age of unconsolidated material, depth to ground water, and peak ground acceleration. Hill (1979) first mapped liquefaction potential in the region using similar methods by implementing a procedure developed by Youd and Perkins (1978)

for liquefaction potential mapping in California based on geologic data. However, the resultant hazard map lacked detail and the rules for defining zone boundaries are specific to Quaternary deposits of California, which Anderson and others (1990a) argue are not relevant to Utah's closed basins.

Anderson and others (1990a) mapped liquefaction potential in our study area by modifying the techniques of Seed and others (1983, 1985), using SPT and CPT data to predict the critical acceleration required to initiate liquefaction. Because geotechnical boreholes were clustered in small, urbanized areas and along major highways, Anderson and others (1990a) devised a method to assess the liquefaction potential in areas lacking geotechnical data. They assessed the geologic and topographic settings of areas with sufficient data to calculate critical accelerations, used these settings to estimate liquefaction potential in areas lacking geotechnical data, and adjusted boundaries after site-specific field checks of geology and topography.

The technique of Anderson and others (1990a), which extends calculated critical accelerations to areas with no geotechnical data based on surficial geologic and topographic similarities, does not specifically consider lateral facies changes within surficial geologic units and the properties of shallow subsurface units. To consider these factors, we use a large database of water-well logs to produce surrogate geotechnical data, supplementing subsurface information from sparse geotechnical boreholes. This procedure assigns numerical values to properties recorded in borehole and well logs that can be associated with tendencies for liquefaction. The sum of numerical values for individual factors indicates relative liquefaction susceptibility which, with surficial geology and calculated values for critical acceleration, we use to define boundaries between zones of different liquefaction potential in our study area (plates 2A through 2D). Our maps therefore estimate the liquefaction hazard by: (1) showing areas in which the potential for liquefaction is increased due to the presence of susceptible soils, and (2) relating the susceptibility to the intensity, probability, and frequency of earthquake ground shaking required to induce liquefaction.

Mapping Procedure

According to Obermeier (1996), the most important factors controlling development of liquefaction are (1) grain size, (2) relative density, (3) depth and thickness of strata, (4) age of sediments, (5) characteristics of the fine-grained cap, (6) topography and nature of seismic shaking, (7) depth to water table, and (8) seismic history. Of these eight factors, three are essentially constant throughout our map area (4–age of sediments, 6–topography and nature of seismic shaking, and 8–seismic history). Of the remaining five factors, one is hydrologic (7–depth to water table) and can be determined from the ground-water map of Bjorklund and McGreevy (1971). Four others are based on strata-specific properties (1–grain size, 2–relative density, 3–depth and thickness of strata, and 5–characteristics of the fine-grained cap) and can be related to subsurface data.

Although liquefaction may occur at depths greater than 20 meters, soil deeper than 15 meters is commonly too deep to liquefy (Seed, 1979). Only 43 of 182 geotechnical boreholes in the central Cache Valley are at least 15 meters deep, and most of these are clustered in Logan. In contrast to the limited depth and irregular spatial distribution of geotechnical boreholes, water wells in the area are

typically deeper than 15 meters and are widely and uniformly distributed. Of 1,032 water wells in the area, 1,014 are at least 15 meters deep. Therefore, we use both geotechnical-borehole and water-well logs to obtain subsurface information related to strata-specific properties within the upper 15 meters of soil.

We subdivide the strata-specific properties into multiple classes based on their association with tendency toward liquefaction, and assign numerical values to each class (table 7). Classes associated with a greater susceptibility to liquefaction are assigned higher values. For each potentially liquefiable layer in a borehole or well, the sum of all five class values is defined as the Total Liquefaction Rating Value (LV). The LV for each well is defined as the highest LV of any layer in the upper 15 meters of that borehole or well. The boundaries between classes within a variable, and the assigned numerical values, are subjective but are based on (1) analogies with the qualitative associations of each variable with liquefaction described in the literature and (2) comparisons between the critical accelerations we computed for selected geotechnical boreholes in the Smithfield quadrangle and the LV for those same boreholes.

Table 7. *Numerical values of factors controlling development of liquefaction assigned to potentially liquefiable layers in water wells.*

Factor	Class	Value
Lithology	Sand	5
	Silt + sand	3
	Clay + sand	2
	Clay + silt + sand	1
	Silt	2
	Sand + gravel	2
	Silt + sand + gravel	1
	Gravel	1
Layer Thickness (meters)	<1.5	4
	1.5-3	3
	3-4.5	2
	>4.5	1
Clay Cap	Yes	4
	No	1
Cap Thickness (meters)	<2	4
	2-4.5	3
	4.5-7.5	2
	>7.5	1
Average Depth of Layer (meters)	<3	8
	3-6	6
	6-9	4
	9-15	2

Obermeier (1996) summarizes the relationship between geologic variables and liquefaction. He notes that liquefaction-induced features often form readily in sand and silty sand and are also documented in gravel and loose silt. However, liquefaction is unusual in sediments containing more

than 15 per cent clay (Seed and others, 1983). Liquefaction generally originates in strata located a few meters to 10 meters beneath the surface, but reported depths range from a few tenths of a meter to greater than 20 meters. Susceptible beds are usually 0.3 to 1.0 meter thick, but are documented to be as thin as 8 to 10 centimeters. Fine-grained, impermeable caps aid liquefaction by preventing dissipation of pore pressure, but Ishihara (1985) observed that liquefied dikes generally do not extend to the surface when the thickness of an overlying impermeable cap exceeds 10 meters and are often severely restricted for thicknesses of more than 5 meters. Liquefaction susceptibility is strongly influenced by depth to ground water with susceptibility decreasing to nil with ground-water depths greater than 10 meters. Liquefaction susceptibility is also indicated by historical liquefaction because liquefaction commonly recurs at the same site.

We supplement the relationships summarized by Obermeier (1996) by comparing critical accelerations we computed for geotechnical boreholes in the Smithfield quadrangle (table 8) with soil properties relevant to liquefaction potential. Comparisons are only provided for layers with critical accelerations less than 0.5 g because layers with greater critical accelerations generally have a very low liquefaction potential. We use this comparison, with the relationships summarized by Obermeier (1996), to define the class boundaries and values shown in table 7. Critical accelerations are computed using equation 16 from Anderson and others (1990a, p. 52):

Eq. 2 $(a_{max})_c = (\tau_{avg}/\sigma'_o)\,(\sigma'_o/\sigma_o)\,(1/0.65r_d)$

where:

$(a_{max})_c$ = critical acceleration to induce liquefaction.

(τ_{avg}/σ'_o) = critical cyclic stress ratio (determined from a relationship with penetration resistance developed by Seed and Idriss, 1982).

σ'_o = initial effective pore pressure (determined from geotechnical-borehole data).

σ_o = total vertical stress (determined from geotechnical-borehole data).

r_d = stress reduction factor (determined from a relationship with depth developed by Seed, 1979).

Liquefiable layers with the lowest critical accelerations in analyzed geotechnical boreholes (shown in table 8) commonly have soil properties related to relatively high liquefaction potential. For example, layers with lower critical accelerations are generally thinner than layers with higher values, consistent with observations of liquefaction of thinner beds by Anderson and others (1990a) at the site of liquefaction during the 1962 Cache Valley earthquake (M_L 5.7) and by Keaton and Anderson (1995) at exposures of prehistorical lateral spreads along the Wasatch Front. Layers with lower critical accelerations are also associated with relatively thin clay caps, again consistent with observations by Anderson and others (1990a). Finally, lower critical accelerations are associated with shallower average depths of liquefiable layers, likely due to consolidation of deeper beds, resulting in increased relative density, higher SPT values, higher shear strength, and greater total

stress. Because this association is particularly strong in our data set, we weight this factor twice as heavily as other factors (table 7). However, boreholes with layers of clayey sand (USCS class SC) are associated with anomalously low critical accelerations, reflecting the lowest average SPT values of all soil types in the Smithfield quadrangle. Because high clay content is associated with a lack of liquefaction susceptibility, SC soils do not warrant a high value for lithology in our rating scheme. Relatively high critical accelerations of well-sorted sands (SP) likely reflect free drainage with resultant greater consolidation from the load of overlying soil.

Table 8. *Characteristics of liquefiable layers in selected geotechnical boreholes in the Smithfield quadrangle with critical accelerations less than 0.5 g.*

Borehole	Critical Acceleration (g)	Lithology (USCS Class)	Layer Thickness (m)	Clay Cap	Cap Thickness (m)	Average Depth of Layer (m)
SBI-11	0.14	SC	0.8	Yes	2.0	2.4
SBI-6	0.23	SM	2.3	Yes	1.7	3.3
SBI-5	0.23	SC	0.9	Yes	2.0	2.4
SBI-2	0.25	SC	0.8	Yes	1.7	2.1
3015-1	0.27	ML-SM	0.8	Yes	2.5	7.3
2017-1	0.31	SP	0.5	Yes	2.6	9.4
SBI-1	0.33	SM-ML	7.0	Yes	2.3	5.8
2017-2	0.33	ML	2.1	Yes	2.4	3.5
SBI-4	0.37	SM-SP	4.1	Yes	2.1	4.2
2017-3	0.37	SP	3.0	Yes	6.6	8.1
SBI-3	0.40	SM-ML	2.9	Yes	1.8	3.3
3015-3	0.48	SM	6.2	Yes	2.6	5.7

We map liquefaction hazards by first computing the Total Liquefaction Rating Values (LV) for geotechnical boreholes and water wells in our study area, using numerical values assigned to factors in table 7. We then use the LVs and surficial geology to map the relative hazard in areas underlain by soil and shallow ground water. Liquefaction-hazard ratings and their criteria are shown in table 9. To define the hazard-rating boundaries, we derive equivalent critical accelerations from maximum considered earthquake peak accelerations on the current USGS National Seismic Hazard Maps (Frankel and others, 1996), using return periods approximately equal to those used by Anderson and others (1990a).

Compute Total Liquefaction Rating Values (LV)

Step 1: From databases containing all geotechnical-borehole and water-well layer data, extract data for all layers with tops less than 15 meters deep.

Step 2: Add the following fields: Clay Cap?, Cap Thickness, Lithology Value, Liquefiable Layer Thickness Value, Clay Cap Value, Clay Cap Thickness Value, Liquefiable Layer Average Depth Value, and Total Value.

Step 3: For each borehole or well, identify the uppermost impermeable clay cap that exists

Table 9. *Characteristics of liquefaction-hazard classifications in the central Cache Valley, Utah.*

Liquefaction Hazard Rating	Hazard-Rating Criteria				Ground Acceleration Required to Induce Liquefaction[4]			Predominant Geology[7]
	Historical Liquefaction[1]	Consolidation (compaction and cementation)	Depth to Ground Water (m)[2]	Liquefaction Value[3]	Equivalent Critical Acceleration (g)[5]	Approximate 50-Year Exceedance Probability (%)[6]	Ground-Motion Return Period (yrs)[6]	
High	Yes	No	<15	n.a.	<0.14	>20	<250	Holocene flood-plain deposits.
Moderate	No	No	<15	>5	0.14-0.28	5 - 20	250 - 1,000	Alluvial levee deposits and Lake Bonneville deposits with granular interbeds; shallow ground-water depth.
Low	No	No	<15	<5	0.28-0.41	2 - 5	1,000 - 2,500	Lake bottom deposits of Lake Bonneville and coarser-grained beds; moderate ground-water depth.
Very Low	No	No	>15	n.a.	>0.41	<2	>2,500	Unconsolidated deposits; deep ground water.
Not Susceptible	No	Yes	n.a.	n.a.	n.a.	n.a.	n.a.	Bedrock.

[1] Sites experiencing liquefaction during the 1962 Cache Valley earthquake are documented in Hill (1979).

[2] Bjorklund and McGreevy (1971).

[3] Areas of moderate and low liquefaction hazard include isolated wells with liquefaction values different than the rating criteria due to the smoothing effect of the GIS interpolation procedure.

[4] Liquefaction is induced in areas with higher liquefaction hazard ratings by lower levels of ground shaking (critical acceleration); lower levels of ground shaking are more likely to occur than are higher levels (exceedance probability) and thus occur more often (return period).

[5] Critical accelerations used by Anderson and others (1990) to define hazard-rating boundaries were calculated from borehole geotechnical data. Our equivalent critical accelerations are derived from maximum considered earthquake peak accelerations mapped by Frankel and others (1996) at the center of our four-quadrangle study area. Ground-motion return periods used to define hazard-rating boundaries are similar to those of Anderson and others (1990).

[6] Ground-motion return periods were chosen to approximate arbitrary values of exceedance probability selected by Anderson and others (1990), who used a 100-year time period to determine exceedance probability. For consistency with USGS national seismic-hazard maps (Frankel and others, 1996) we use a 50-year time period.

[7] Boundaries of hazard areas do not coincide with geologic map units except for the high-hazard area, which includes geologic units known to have experienced liquefaction during historical earthquakes.

n.a.–not applicable.

immediately above a liquefiable layer (possible lithologies of liquefiable layers are listed in table 7). If a clay cap exists, enter Y in the *Clay Cap?* field of the underlying liquefiable layer; if more than one liquefiable layer is overlain by clay, enter Y only in the *Clay Cap?* field of the liquefiable layer directly beneath the uppermost clay cap. For all other liquefiable layers, enter N.

Step 4: For liquefiable layers directly beneath the uppermost clay cap (identified with Y in the *Clay Cap?* field), enter the thickness of the clay cap in the *Cap Thickness* field.

Step 5: From the database containing layers with tops less than 15 meters deep, extract records for layers that contain potentially liquefiable lithologies listed in table 7 (these are the layers identified either with Y or N in the *Clay Cap?* field).

Step 6: Join the resulting database to a polygon map of depth to ground water, where polygons represent 0.3-meter depth contours of the water table. For the central Cache Valley, we derive 0.3-meter depth contours by interpolating between contours with larger intervals mapped by Bjorklund and McGreevy (1971). Do not use static water depths listed on borehole or well logs because these may be influenced by artesian aquifers.

Step 7: From the database containing potentially liquefiable layers with tops less than 15 meters deep, extract records for layers with tops beneath the water table.

Step 8: Update the five value fields in the resulting database (*Lithology Value*, *Liquefiable Layer Thickness Value*, *Clay Cap Value*, *Clay Cap Thickness Value*, and *Liquefiable Layer Average Depth Value*) with values from table 7.

Step 9: Sum the five values for each layer in the *Total Value* field.

Step 10: In a mappable database that contains general location information on each borehole and well (one record for each borehole or well), create a new field named *Liquefaction Value*. Update that field with data from *Total Value* in the liquefaction database.

Step 11: For boreholes or wells with more than one liquefiable layer, ensure that the layer with the highest *Total Value* is used for the *Liquefaction Value* in that borehole or well.

Step 12: For boreholes or wells with no liquefiable layers, enter 0 for the *Liquefaction Value*.

Map Liquefaction Hazards

Step 1: Assign a rating of Non-Susceptible Bedrock to bedrock map units to signify that these materials are consolidated and the approach outlined above is not applicable.

Step 2: Assign a rating of Very Low to unconsolidated surficial units with ground water deeper than 15 meters. This reflects the rarity of documented liquefaction in saturated layers beyond this

depth.

Step 3: In areas not assigned a hazard rating in steps 1 and 2, interpolate a grid of regularly spaced LVs from the irregularly spaced borehole and well data. Parameters for interpolation may vary depending upon the characteristics of data within a particular study area. For the central Cache Valley, we use a cell size of 80 meters and an Inverse Distance Weighting algorithm. The LV at each grid cell was computed based on the weighted average of all values within a 2,000-meter radius of the grid cell, using a distance-weighted exponent of –2.

Step 4: Contour LV for all geotechnical boreholes and water wells at least 15 meters deep at a value of 5. Assign ratings of Low to areas with liquefaction values less than 5 and Moderate to areas with liquefaction values greater than 5. We use a liquefaction value of 5 as a boundary between Low and Moderate liquefaction-potential zones to ensure that all areas with susceptible layers are included in the Moderate zone, and only those areas lacking susceptible layers are in the Low zone. Also, higher values define an increasing number of small, isolated areas and lower values are insufficient to adequately differentiate distinct areas of hazard potential that approximate the pattern mapped by Anderson and others (1990a).

Step 5: Within each of the major areas of hazard potential, remove small, isolated areas of anomalous hazard potential because their inclusion represents a level of detail not supported by the inherent uncertainties of water-well data.

Step 6: Assign a rating of High to unconsolidated surficial units known to have experienced liquefaction during historical earthquakes. In the central Cache Valley, Hill (1979) reported liquefaction during the 1962 M_L 5.7 Cache Valley earthquake in Holocene flood-plain deposits.

Step 7: Modify the hazard rating of areas underlain by geologic units known to have experienced historical liquefaction (step 6) based on observation of sediment texture and ground-water depth. This step is necessary because the extent of historical liquefaction may be limited to a small part of the total area underlain by the geologic unit that was subject to liquefaction. In the central Cache Valley, for example, liquefaction occurred in sandy Holocene flood-plain deposits of the Bear River, but flood-plain deposits of the Logan River and Blacksmith Fork (plate 2D) contain significant amounts of gravel and are less susceptible to liquefaction. We therefore progressively reduce the hazard rating of these flood plains from high near the center of the valley where flood-plain deposits are mostly sandy, to moderate as the drainages rise in elevation on the piedmont slope where the proportion of gravel (observed in outcrop but apparently absent in water wells with an LV of 0) increases, to low in the upper reaches of the drainages where the thickness of susceptible beds is minimal but ground water depth is shallow as shown by the presence of perennial stream flow. We make similar adjustments to the hazard rating of flood plains draining Providence and Smithfield Canyons.

Step 8: All hazard ratings except for moderate are defined on the basis of criteria other than the presence of susceptible layers assigned liquefaction values (not susceptible - bedrock; very

low - deep ground water; low - shallow ground water but no susceptible layers; high - historical liquefaction). Label all borehole and well locations in moderate-hazard areas with their liquefaction values to indicate the relative susceptibility of soil to liquefaction.

Determine Equivalent Critical Accelerations

Anderson and others (1990a) defined the boundaries of their liquefaction-potential zones by critical accelerations that have a certain probability of nonexceedance within a 100-year period. They compared these to calculated critical accelerations from geotechnical-borehole data. We derive equivalent critical accelerations from maximum considered earthquake peak accelerations on the current USGS National Seismic Hazard Maps (Frankel and others, 1996) at the center of our four-quadrangle study area and use these figures to define hazard-rating boundaries similar to those of Anderson and others (1990a). However, Frankel and others (1996) map ground accelerations based on a 50-year period, rather than 100 years. We therefore estimate equivalent critical accelerations from the map of Frankel and others (1996) by using comparable return periods.

The critical accelerations used as zone boundaries by Anderson and others (1990a) (0.1 g between high and moderate liquefaction potential, 0.18 g between moderate and low, and 0.25 g between low and very low) have respective return periods of 200, 1,000, and 2,000 years (table 10). The maps of Frankel and others (1996) have return periods of 500, 1,000, and 2,500 years. The 500-year return period is much longer than the 200-year return period used by Anderson and others (1990a) for the boundary between high and moderate liquefaction potential, but the return periods for other zone boundaries are similar. From Frankel and others (1996), the acceleration with a comparable return period to the boundary between moderate and low liquefaction potential of Anderson and others (1990a) is 0.28 g, and the acceleration with a comparable return period to the boundary between low and very low liquefaction potential is 0.41 g. We can estimate that the acceleration with a return period of 200 to 250 years, based on the latest USGS prediction of 0.28 g for peak ground acceleration for a 1,000-year return period for this location, would be about 0.14 g (about half of 0.28 g). Thus, our values for acceleration for equivalent return periods are somewhat higher than values used by Anderson and others (1990a), but Keaton and Anderson (1995) acknowledge that values should be higher based on the results of much recent research released after earlier liquefaction studies were completed.

Table 10. *Liquefaction potential related to critical acceleration for liquefaction-hazard mapping in the central Cache Valley.*

Liquefaction Potential	Anderson and others, 1990a		This Study	
	Critical Acceleration (g)	Ground-Motion Return Period (years)	Equivalent Critical Acceleration (g)	Ground-Motion Return Period (years)
High	<0.1	<200	<0.14	<250
Moderate	0.1-0.18	200-1,000	0.14-0.28	250-1,000
Low	0.18-0.2	1,000-2,000	0.28-0.41	1,000-2,500
Very Low	>0.25	>2,000	>0.41	>2,500

Results

Our mapped pattern of liquefaction-hazard potential is similar to that of Anderson and others (1990a). We map the highest potential for liquefaction in the flood plains of the Bear, Little Bear, and Logan Rivers in the center of the valley (plates 2A, 2C, and 2D). This potential reflects the presence of saturated, loose, sandy Holocene alluvial sediments. Historical liquefaction occurred in these deposits along the Bear River during the 1962 Cache Valley earthquake. Anderson and others (1990a) note that flood-plain soils are proportionately sandier north of Logan and therefore mostly assign a high hazard potential to flood plains north of Logan and a moderate to high hazard potential to flood plains south of Logan. We do not make this distinction because we prefer a more conservative interpretation of the liquefaction potential of the flood-plain deposits, which are generally sandy in both areas.

We map a moderate potential for liquefaction on much of the valley floor adjacent to the Bear and Logan Rivers and Cutler Reservoir. In this area, sand and silt are common in middle Holocene to late Pleistocene alluvial-levee deposits adjacent to the Bear River and granular interbeds occur within offshore, finer grained latest Pleistocene Lake Bonneville deposits. Ground water is close enough to the ground surface that most granular beds are saturated and susceptible to liquefaction. Our area of moderate liquefaction potential is more extensive than that of Anderson and others (1990a) because we identify susceptible beds on water-well logs in areas where Anderson and others (1990a) relied upon the characteristics of surficial geologic units.

We map a low potential for liquefaction on the remainder of the valley floor at the distal parts of piedmont slopes. This reflects the increasing depth of ground water on the valley margin. Departures from the mapping of this category by Anderson and others (1990a) occur in the southwest part of our study area near Wellsville west of the Bear River (plate 2C), and in the northwest part of our study area near Newton north of Cutler Reservoir (plate 2A). Anderson and others (1990a) map a very low hazard potential in these areas but we note a significant proportion of granular material in water wells of these areas that, despite relatively deep ground water, represents a higher (although still low) hazard potential. Granular material is also noted in the description of surficial geologic units mapped in these two areas by Solomon (1999), who maps Lake Bonneville sand and silt near Wellsville and middle Holocene to uppermost Pleistocene alluvium near Newton.

We map a very low potential for liquefaction on the upper part of piedmont slopes and valley-margin benches on the east side of the valley and near Little Mountain in the northwest corner of the study area. These deposits, including coarse-grained alluvial and nearshore Lake Bonneville material, do not pose a significant liquefaction hazard despite their grain size because ground water in these areas is normally deeper than 15 meters. However, our hazard map is based upon the depth of ground water at the time that our data source (Bjorklund and McGreevy, 1971) was compiled. Ground-water depth varies with time and ground water may be locally perched at shallow depths above impermeable beds. Should ground-water depth decrease in these areas, liquefaction-hazard potential would increase. Our distribution of areas with very low potential for liquefaction is similar to that mapped by Anderson and others (1990a) on the east side of the valley but, because Bjorklund and McGreevy (1971) indicate that ground-water is generally less than 15 meters deep on the west

side of the valley, we map a low to moderate liquefaction potential on upper piedmont slopes of that area rather than the very low potential mapped by Anderson and others (1990a).

Our maps provide a regional assessment of liquefaction hazards in the central Cache Valley, but care should be used for proper application of the mapping techniques and data. We use data from water wells because they are more widespread than geotechnical boreholes in our study area. However, geologic interpretations based on water-well logs are less precise than interpretations of borehole logs. The use of water-well logs is appropriate only for regional studies in areas where geotechnical data are sparse or lacking. Water-well logs should not be relied upon for site-specific investigations. Our recommendations for the need to conduct site-specific investigations are shown in table 6.

EARTHQUAKE-INDUCED SLOPE-FAILURE HAZARDS

Downslope movements of rock or soil under the influence of gravity may be triggered by earthquake ground shaking. The Oregon Department of Geology and Mineral Industries (Keefer and Wang, 1997; Hofmeister, 1999a, 1999b) map regional earthquake-induced slope-failure hazards in three groups: (1) lateral spreads on gentle soil slopes, (2) translational landslides on moderate soil slopes, and (3) failures of rock slopes. Lateral spreads are characterized by surficial blocks of sediment which are displaced laterally down gentle slopes as a result of liquefaction in a subsurface layer. Translational landslides are characterized by one or more discrete blocks of sediment which are displaced down moderate slopes on a generally planar surface of rupture in weak material. Rock-slope failures are characterized by the downslope movement of intact bedrock and weathered residual material that retain significant components of original rock structure.

We map earthquake-induced slope-failure hazards in the central Cache Valley by modifying the Oregon techniques to reflect recent changes in empirical equations used to predict landslide displacements (plates 3A through 3D). We also modify the range of slopes analyzed for translational and rock-slope landslides to reflect our uncertainty of soil thickness on rock slopes and revise hazard classifications to ensure prudent development on steep slopes. We calculated the displacement expected from lateral spreads using the empirical equation of Youd and others (1999), a revision of an equation first developed by Bartlett and Youd (1992) from observations at sites of historical lateral spreading. To estimate values of geotechnical parameters needed for input into the equation we applied methods developed by Mabey and others (1993) for mapping earthquake hazards in Portland, Oregon. We calculated Newmark displacements, a relative measure of the potential for translational landslides, using the empirical equation of Jibson and others (1998) determined from data collected during and after the 1994 Northridge, California earthquake. This relationship is a modification of an equation published earlier by Jibson (1993). We assessed the stability of rock slopes using the method of Keefer (1993), based on associations between landslide concentrations and slope characteristics documented from historical earthquakes.

Mapping Procedure

Map Lateral-Spread Hazards on Gentle Soil Slopes

Bartlett and Youd (1992) developed empirical equations that relate the lateral ground displacement observed at 450 sites of historical lateral spreading to six parameters. They developed two models, one for areas near incised streams or steep banks (the free-face model) and another for areas with relatively uniform and gentle ground slopes (the ground-slope model). Youd and others (1999) revised the equations by incorporating several modifications into their functional form and enlarging the data set used to establish correlations between parameters.

For free-face conditions, the formula of Youd and others (1999, equation 4a) is:

Eq. 3 $\text{Log } D_H = -18.084 + 1.581\ M - 1.518\ \text{Log } R^* - 0.011\ R + 0.551\ \text{Log } W + 0.547\ \text{Log } T_{15} + 3.976\ \text{Log } (100 - F_{15}) - 0.923\ \text{Log } (D50_{15} + 0.1)$

For ground-slope conditions, the formula of Youd and others (1999, equation 4b) is:

Eq. 4 $\text{Log } D_H = -17.614 + 1.581\ M - 1.518\ \text{Log } R^* - 0.011\ R + 0.343\ \text{Log } S + 0.547\ \text{Log } T_{15} + 3.976\ \text{Log } (100 - F_{15}) - 0.923\ \text{Log } (D50_{15} + 0.1)$

where:

D_H = estimated lateral ground displacement, in meters.

M = earthquake moment magnitude.

$R^* = R + Ro$

R = horizontal distance from the seismic energy source, in kilometers.

$Ro = 10^{(0.89M-5.64)}$

W = free-face ratio, defined as the height (H) of the free face divided by the distance (L) from the base of the free face to the point in question, in percent.

S = ground slope, in percent.

T_{15} = cumulative thickness of saturated granular layers in the upper 15 meters of soil with corrected blow counts, $(N_1)_{60}$, less than 15, in meters.

F_{15} = average fines content (percent passing a no. 200 sieve) of saturated granular layers included in T_{15}.

$D50_{15}$ = average mean grain size of sediments within layers included in T_{15}, in

millimeters.

To apply the formula for free-face conditions, free faces must be steep (near vertical). In our study area, most free faces (the highest of which are along the Bear River) are grassy and below the angle of repose. The highest, steep free face is 5 meters high on the south bank of Cutler Reservoir in the northwest part of the Newton quadrangle (plate 3A). At a distance of 60 meters from the base of this free face, the minimum distance we consider for mapping the lateral-spread hazard (one-tenth of map scale), the free-face ratio (W) is 7.5 percent. At this location, the ground slope (S) is 2 percent. Substituting these values in the equations of Youd and others (1999) results in similar values for lateral ground displacements under both conditions, and ground displacement due to free-face conditions rapidly decreases with increasing distance from the free face. Thus, lateral ground displacement due to ground-slope conditions is predominant in the central Cache Valley, lateral ground displacement due to free-face conditions is not significant at the map scale, and we do not analyze lateral spreading under free-face conditions. However, displacement due to free-face conditions should be considered where appropriate for site-specific investigations, such as in areas near incised streams or steep embankments.

The ground-slope equation of Youd and others (1999) requires values for earthquake magnitude (M), distance to the earthquake source (R), and texture of liquefiable sediments (F_{15} and D_{15}). For this study, we assume an earthquake of magnitude 6.5 occurs at a constant distance of 5 kilometers from each map point, resulting in calculated values of 1.4 for Ro and 6.4 for R*. The map therefore does not estimate lateral-spread displacements resulting from an earthquake with a particular return period, but estimates displacements for the given earthquake and represents the relative hazard for other conditions. We also assume an average fines content of 30 percent and an average mean grain size of 0.2 millimeters. These values match those used by Mabey and others (1993) in their analysis of lateral spreading in Holocene alluvium of the Portland, Oregon 7.5-minute quadrangle, and reflect the lack of data on sediment texture in our study area. Using these values, the ground-slope equation simplifies to:

Eq. 5 $\text{Log } D_H = -0.797 + 0.343 \text{ Log } S + 0.547 \text{ Log } T_{15}$

The ground-slope equation also requires values for ground slope (S) and the thickness of saturated granular layers (T_{15}). Ground slope is obtained from USGS digital elevation models (DEMs). The thickness of saturated granular layers is obtained by first identifying all granular layers less than 15 meters deep with SPT values less than 15 in geotechnical boreholes (exclude layers with USCS classes of PT, OH, OL, CH, CL, and GC). We then calculate the average thickness of these layers for each surficial-geologic map unit drilled by the boreholes (table 11) and, because boreholes are sparse and irregularly distributed in the central Cache Valley (table 1), we estimate the thickness of granular layers in units not drilled by comparison with units of similar texture having subsurface data. This represents the thickness of granular layers that is potentially available for liquefaction (table 12). We can estimate the proportion of that material that is saturated by ground water and therefore predict the thickness of saturated granular layers, by the following equation:

Eq. 6 $\text{Predicted } T_{15} = (\text{Potential } T_{15})((15\text{-GWdepth})/15)$

where:

Predicted T_{15} = predicted cumulative thickness of saturated granular layers with corrected blow counts, $(N_1)_{60}$, less than 15, in meters.

Potential T_{15} =potential cumulative thickness of saturated granular layers with corrected blow counts, $(N_1)_{60}$, less than 15, in meters.

GWdepth = depth to water table, in meters. For the central Cache Valley, we use the polygon map of depth to ground water derived from Bjorklund and McGreevy (1971) to map liquefaction hazards.

Table 11. *Cumulative thickness of granular layers with blow counts, $(N_1)_{60}$, less than 15 in the upper 15 meters of geotechnical boreholes drilled in surficial geologic-map units.*

Geologic Units	Number of Boreholes	Minimum Thickness (m)	Maximum Thickness (m)	Average Thickness (m)
Lake Bonneville silt and clay	10	0.3	6.4	1.6
Undivided lacustrine, marsh, and alluvial deposits	4	0.6	4.6	2.5
Stream alluvium (upper Holocene)	6	0.3	4.7	2.6
Stream alluvium, undivided (Holocene to uppermost Pleistocene)	5	0.7	5.7	2.9
Lake Bonneville sand and silt	10	0.8	5.0	3.0
Alluvial sand and silt of natural levees	9	1.1	7.8	4.3
Lake Bonneville deltaic deposits	7	0.8	11.6	6.1

Table 12. *Potential cumulative thickness of granular layers with blow counts, $(N_1)_{60}$, less than 15 in the upper 15 meters of soil underlying surficial geologic-map units on gentle soil slopes.*

Geologic Units	Potential T_{15} (m)
Thin Lake Bonneville sand and gravel overlying fan alluvium	1.0
Lake Bonneville silt and clay	1.5
Undivided lacustrine, marsh, and alluvial deposits	2.5
Fan and stream alluvium Undivided colluvium and alluvium Lake Bonneville sand and silt	3.0
Alluvial sand and silt of natural levees	4.5
Lake Bonneville gravel, sand, and deltaic deposits	6.0

With the necessary unknowns now quantified, we map the lateral-spread hazard on slopes less than 6 percent, the maximum gradient of slope failures evaluated by Bartlett and Youd (1992).

Step 1: Make a slope map from the USGS DEM. Normally, the 30-meter DEM should be used for a 1:24,000-scale map. However, the 30-meter DEMs for the Logan, Smithfield, and Wellsville quadrangles are defective, exhibiting an east-west striping. We therefore used the 90-meter DEMs. These also are defective, exhibiting a striping parallel to valley contours, but erroneous interpretations were easier to resolve at this scale.

Step 2: From the slope map, create a point vector database for slopes (in percent) within each grid cell.

Step 3: Remove all records except for those with slopes less than 6 percent.

Step 4: Update the database by adding a column for geologic-map unit.

Step 5: Remove all records for bedrock units.

Step 6: Update the database by adding a column for ground-water depth from the polygon map of depth to ground water created to map liquefaction hazards.

Step 7: Update the database by assigning a value of 0 to estimated lateral ground displacement (D_H) for all cells where ground-water depth is greater than 15 meters.

Step 8: Update the database by assigning values for Potential T_{15} to each cell where ground-water depth is less than 15 meters, based on geologic-map unit. Values for the central Cache Valley are shown in table 12.

Step 9: Update the database by calculating values for Predicted T_{15} using values for ground-water depth (step 6) and Potential T_{15} (step 8) in equation 6.

Step 10: Update the database by calculating values for Log D_H using values for slope (step 2) and Predicted T_{15} (step 9) in equation 5.

Step 11: Update the database by calculating D_H, in meters, taking the antilog (10^Log D_H) of values from step 10.

Step 12: Produce a grid of D_H using values from steps 7 and 11.

Step 13: Smooth the grid of D_H by interpolation. Parameters for interpolation may vary depending upon the characteristics of data within a particular study area. For the central Cache Valley, we use an Inverse Distance Weighting algorithm based on the weighted average of all values within a 2,000-meter radius of the grid cell and a distance-weighted exponent of –2.

Step 14: Contour the grid at 0.1, 0.2, and 0.3 meters. This creates four hazard classifications defined by the amount of lateral ground displacement (table 13). The classifications are Very Low (less than 0.1 meters), Low (0.1-0.2 meters), Moderate (0.2-0.3 meters), and High (greater than 0.3 meters). These intervals are related to the degree of building damage that may be expected to occur from lateral spreading during earthquakes according to Youd (1980).

Table 13. *Characteristics of lateral-spreading hazard classifications.*

Slope-Failure Hazard	Lateral Ground Displacement (cm)[1]	Depth to Ground Water (m)[2]	Expected Damage[3]	Predominant Geology[4]
High	>30	<15	Severe damage or collapse, nonrepairable	Alluvial-levee and flood-plain deposits; Lake Bonneville nearshore and deltaic deposits; existing landslides.
Moderate	20-30	<15	Severe damage, repairable	Alluvial-levee, flood-plain, and fan deposits; Lake Bonneville nearshore and lake-bottom deposits.
Low	10-20	<15		Lake Bonneville lake-bottom and nearshore deposits.
Very Low	<10	<15 on very gentle slopes or >15 on all slopes	Little damage, repairable	Unconsolidated deposits.

[1] Lateral displacements are valid only for the conditions assumed in the analysis. Displacements will vary with different earthquake magnitudes, distance to seismic sources, textures of liquefiable sediments, and ground-water depth. For this study, assumed conditions include an earthquake magnitude of 6.5, a distance of 5 km to the seismic source, and liquefiable sediments consisting of silty sand with a fines content of 30% and a mean grain size of 0.2 mm. Site-specific investigations are required to determine accurate sediment textures and ground-water depth.

[2] Bjorklund and McGreevy (1971).

[3] Youd (1980).

[4] Boundaries of hazard areas do not coincide with geologic map units except for Tertiary units in very-high-hazard areas and existing landslides in high-hazard areas.

Step 15: Assign a classification of High to existing landslides, regardless of the estimated lateral ground displacement.

Step 16: Within each of the major areas of hazard potential, remove small, isolated areas of anomalous hazard potential because their inclusion represents a level of detail not supported by the inherent uncertainties of the data.

Map Translational-Landslide Hazards on Moderate Soil Slopes

GIS techniques to predict seismic slope instability on moderate to steep soil slopes commonly include pseudostatic (Keaton and others, 1987; Mabey and others, 1993), Newmark (Wieczorek and others, 1985), or modified Newmark (McCalpin, 1996) methods. All of these methods work best where infinite-slope failures predominate. Infinite-slope failures occur when a shallow slip surface is

parallel to the slope. This condition predominates in granular Lake Bonneville deposits near the valley margin, where shoreline deposits failed as shallow debris slides and deltaic deposits failed after springs saturated basal gravel beds overlying impermeable strata exposed in steep stream embankments.

An approach using modified Newmark methods was suggested by Jibson (1993), who established an empirical relationship between Arias intensity (a comprehensive and quantitative measure of total shaking intensity developed by Arias, 1970) and Newmark displacement (a method of analysis that calculates the cumulative permanent displacement of a sliding block as it is subjected to the effects of an earthquake acceleration-time history, proposed by Newmark, 1965). The Oregon Department of Geology and Mineral Industries (Keefer and Wang, 1997; Hofmeister, 1999a, 1999b) map landslide hazards on moderate soil slopes by calculating Newmark displacements using the Jibson (1993) approach. They apply this technique on slopes ranging from 5 to 25 degrees, including slopes underlain by bedrock, assuming that bedrock slopes are mantled by colluvium. We calculate Newmark displacements on moderate soil slopes using the empirical equation of Jibson and others (1998), a modification of the equation presented by Jibson (1993) determined from data collected during and after the 1994 Northridge, California earthquake. However, we apply this technique only on slopes greater than 6 percent (3.5 degrees), the maximum slope for which we map lateral-spread hazards. We also only apply this technique on slopes that are not underlain by bedrock because we assume that colluvium is thin on rock slopes and apply the method of Keefer (1993) to assess their stability. The stability of rock slopes is addressed in the next section of this report.

The empirical equation of Jibson and others (1998) is:

Eq.7 $\text{Log } D_n = 1.521 \text{ Log } I_a - 1.993 \text{ Log } a_c - 1.546$

where:

D_n = Newmark displacement, in centimeters.

I_a = Arias intensity, in meters per second.

a_c = Critical acceleration, in g.

Equation 7 requires values for Arias intensity (I_a) and critical acceleration (a_c). Jibson (1993) presents two additional equations that we combine to calculate Arias intensity. The first equation (developed by R.C. Wilson, U.S. Geological Survey, using strong-motion records) is a function of the duration of strong ground shaking and probabilistic peak ground acceleration:

Eq. 8 $I_a = 0.9Ta^2$

where:

T = Dobry duration (the time required to build up 90 percent of the Arias intensity), in seconds.

a = peak ground acceleration (PGA), in g.

The second equation (developed by Dobry and others, 1978) allows us to calculate the duration of strong ground shaking from an estimated value for earthquake magnitude:

Eq. 9 $\text{Log } T = 0.432M - 1.83$

where:

M = earthquake magnitude (unspecified, but we assume moment magnitude).

Combining the two equations creates a third relationship that permits us to calculate Arias intensity from peak ground acceleration and earthquake moment magnitude:

Eq. 10 $I_a = 0.9(10^{0.432M-1.83})a^2$

The PGA with a 10 percent probability of exceedance in 50 years at the center of our study area is 0.2 g. Because this value assumes contributions from multiple sources (including the Wasatch, West Cache, and East Cache fault zones), we cannot precisely define the magnitude of the earthquake that controls the PGA without performing a formal deaggregation analysis. However, we can estimate this magnitude by considering earthquakes from local sources that may reasonably be expected during the return period corresponding to the PGA. A PGA with a 10 percent probability of exceedance in 50 years has a return period of about 500 years. The minimum return period for local faults is about 1,300 years for the Brigham City segment of the Wasatch fault zone (McCalpin and Nishenko, 1996) and maximum paleoearthquake magnitudes for local faults are at least M_W6.9. The largest historical earthquake in the region had a magnitude of M_L 5.7. We therefore estimate that the magnitude of an earthquake corresponding to a PGA with a 10 percent probability of exceedance in 50 years at the center of our study area lies about midway between these two extremes and is about 6.5. Using values of M = 6.5 and a = 0.2 g in equation 10 yields a value of I_a = 0.342 meters/second, and equation 7 simplifies to:

Eq. 11 $\text{Log } D_n = -2.255 - 1.993\text{Log } a_c$

Equation 11 requires a value for critical acceleration (a_c). Newmark (1965) showed that the critical acceleration of a potential landslide is a function of the static factor of safety and the landslide geometry:

Eq. 12 $a_c = (SFS-1)\text{Sin}\alpha$

where:

SFS = static factor of safety.

α = thrust angle (the angle from the horizontal that the center of mass of the potential landslide block first moves).

For a planar slip surface parallel to the slope (an infinite slope), the thrust angle is the slope angle, which we can measure from slope maps derived from USGS digital elevation models. We calculate the static factor of safety with the following formula:

Eq. 13 $SFS = (c + 5(d - 62.4m)(Tan\phi)(Cos(s^2)))/((5dSin(s))(Cos(s)))$

where:

c = cohesion of slope materials, in pounds/square foot.

d = dry density of slope materials, in pounds/cubic foot.

m = proportion of a 5-foot (1.5-meter) thick infinite slab of slope materials that is saturated, ranging from 0 to 1.

ϕ = angle of internal friction, in radians.

s = slope angle, in radians.

The following procedure uses equation 13 to calculate static factors of safety, which are then applied to equation 12 to determine critical accelerations. Next, critical accelerations are used to solve equation 11 for Newmark displacement.

Step 1: Make a slope map from the USGS DEM.

Step 2: From the slope map, create a point vector database for slopes (in percent) within each grid cell.

Step 3: Remove all records except for those with slopes greater than 6 percent.

Step 4: Update the database by adding a column for geologic-map unit.

Step 5: Remove all records for bedrock units.

Step 6: Update the database by assigning values for cohesion of slope materials (in pounds per square foot), angle of internal friction of slope materials (in degrees), and dry density of slope materials (in pounds per cubic foot) to each cell based on geologic-map unit. Estimated values for the central Cache Valley are shown in table 14, but these values are based on only a few actual measurements and are thus coarse approximations.

Step 7: Update the database by converting values for slope from percent to radians and friction angle from degrees to radians.

Step 8: Update the database by adding a column f ground-water depth. The column will contain

ranges of ground-water depth, obtained by joining the database to a polygon map of depth to ground water. For the central Cache Valley, this map consists of polygons bounded by the contours mapped by Bjorklund and McGreevy (1971) rather than polygons representing 0.3-meter depth contours created to map liquefaction hazards. We use ranges to account for the uncertainty of the degree of saturation when calculating the SFS of an infinite slab. Ranges of ground-water depth are shown in table 15.

Table 14. *Geotechnical properties of Quaternary geologic-map units on moderate soil slopes, derived from subsurface measurements and data for similar lithologies cited in the literature.*

Geologic Units	Cohesion (psf)	Friction Angle (°)	Dry Density (pounds/ft^3)
Stream alluvium (late Holocene)	0	35	64
Stream alluvium (middle Holocene to uppermost Pleistocene) Stream alluvium (Holocene to uppermost Pleistocene, undivided)	0	35	91
Stream alluvium (uppermost Pleistocene)	0	35	95
Lake Bonneville gravel and sand Lake Bonneville deltaic deposits related to the Provo and younger shorelines	0	35	115
Rock-fall deposits	0	40	115
Alluvial sand and silt of natural levees	880	30	89
Fan alluvium (middle Holocene to uppermost Pleistocene) Fan alluvium (Holocene to uppermost Pleistocene, undivided)	1,740	35	114
Colluvium	1,800	30	90
Lake Bonneville sand and silt	1,800	30	94
Undivided colluvium and alluvium	1,800	30	95
Fan alluvium (late Holocene)	1,940	35	108
Debris-flow deposits	2,000	35	95
Fan alluvium (middle Pleistocene)	2,000	35	115
Lake Bonneville deltaic deposits related to the Bonneville shoreline	2,100	35	94
Undivided lacustrine, marsh, and alluvial deposits	2,200	0	76
Lake Bonneville silt and clay	2,260	0	94

Table 15. *Inferred proportion of a 5-foot (1.5-meter) thick infinite slab of slope materials that is saturated (*m *in equation 13).*

Ground-Water Depth (Bjorklund and McGreevy, 1971) (meters)	Inferred Proportion of Saturation
At or above the land surface	1
0 to 3	0.5
3 to 15	0.1
> 15	0

Step 9: Update the database by adding a column for the inferred proportion of saturation of a 5-foot (1.5 meter) thick infinite slab of slope materials (m in equation 13) (table 15). We assume

that in areas with ground-water depth (determined in step 8) at or above the ground surface the slab is completely saturated (m = 1) and in areas with ground-water depth greater than 15 meters the slab is dry (m = 0). To account for fluctuations in ground-water depth, we assume that the lower half of the slab is saturated in areas with ground-water depth from 0 to 3 meters (m = 0.5) and the lower 10 percent of the slab is saturated in areas with ground-water depth from 3 to 15 meters (m = 0.1).

Step 10: Update the database by calculating values for the static factor of safety (SFS) for a 5-foot (1.5-meter) thick slab, using values for cohesion of slope materials (step 6), dry density of slope materials (step 6), angle of internal friction (step 7), slope angle (step 7), and proportion of a 5-foot (1.5-meter) thick infinite slab of slope materials that is saturated (step 9) in equation 13.

Step 11: Update the database by calculating values for critical acceleration (a_c) using values for the thrust angle (equivalent to the slope angle, step 7) and the static factor of safety (step 10) in equation 12.

Step 12: Update the database by calculating values for Log D_n using values for critical acceleration (step 11) in equation 11.

Step 13: Update the database by calculating the Newmark displacement (D_n), in centimeters, taking the antilog (10^Log D_n) of values from step 12.

Step 14: Produce a grid of D_n using values from step 13.

Step 15: Smooth the grid of D_n by interpolation. Parameters for interpolation may vary depending upon the characteristics of data within a particular study area. For the central Cache Valley, we use an Inverse Distance Weighting algorithm based on the weighted average of all values within a 90-meter radius of the grid cell and a distance-weighted exponent of –2.

Step 16: Contour the grid at 3, 6, and 10 centimeters. This creates four hazard classifications defined by the amount of Newmark displacement (table 16). The classifications are Very Low (less than 3 centimeters), Low (3-6 centimeters), Moderate (6-10 centimeters), and High (greater than 10 centimeters). These intervals are related to observed displacement of landslides resulting from historical earthquakes. For example, Schuster and Chleborad (1990) inventoried ground cracking and landslides from the 1949 and 1965 earthquakes in Puget Sound, Washington, and concluded that cracks with apertures from 10 to 20 centimenters were common, but beyond that width were virtually absent, suggesting that movement within this range triggered catastrophic landsliding. Keefer and Wilson (1989) used 10 centimeters as the critical displacement for coherent landslides in southern California and Wieczorek and others (1985) used 5 centimeters as the critical displacement leading to macroscopic ground cracking and landslide failure in San Mateo County, California.

Step 17: Assign a classification of High to existing landslides, regardless of the Newmark

displacement.

Table 16. *Characteristics of translational-landsliding hazard classifications.*

Slope-Failure Hazard	Newmark Displacement (cm)[1]	Expected Deformation	Predominant Geology[2]
High	>10	Slab failure likely.	Existing landslides.
Moderate	6-10	Slab failure possible, ground cracking likely.	n.a.
Low	3-6	Ground cracking.	
Very Low	<3	Deformation unlikely.	Unconsolidated deposits on piedmont slopes and in mountain canyons.

[1] Predicted Newmark displacements do not necessarily correspond directly to measurable slope movements in the field; they are a relative measure of field performance. The calculated displacements are only valid for the conditions assumed in the analysis. Displacements will vary with different earthquake magnitudes, peak ground accelerations, soil properties, and ground-water depth. For this study, assumed conditions include an earthquake magnitude of 6.5, a peak ground acceleration of 0.2 g (corresponding to a 10% probability of exceedance in 50 years), and representative values for shear strength and dry density of slope materials within each surficial-geologic unit. Site-specific investigations are required to determine accurate soil properties and ground-water depth.

[2] Boundaries of hazard areas do not coincide with geologic map units except for existing landslides in high-hazard areas.

n.a.–not applicable.

Step 18: Within each of the major areas of hazard potential, remove small, isolated areas of anomalous hazard potential because their inclusion represents a level of detail not supported by the inherent uncertainties of the data.

Map Bedrock-Slope-Failure Hazards

Keefer (1993) presents a method for assessing the seismic stability of rock slopes using existing maps and reports, aerial photographs, and reconnaissance-level field observations. The method, based on observed associations between landslide concentrations and slope characteristics in 24 historical earthquakes that occurred in various regions, revises assessment criteria in Keefer and others (1979), Wilson and Keefer (1985), and Keefer and Wilson (1989). Keefer (1993) applies the method to all rock-slope failures, but 90 percent of the earthquake-induced landslides that he studied were rock falls and rock slides. Therefore, the method is more applicable to those types of rock-slope failures. Keefer (1993) defines rock slopes as all slopes designated as bedrock on geologic maps, including intact bedrock, poorly consolidated materials, intensely weathered residual materials, and residual soils less than about 1 meter thick.

Because direct measurement of geotechnical parameters required to analyze rock-slope stability is often not conducted during or following earthquakes, Keefer (1993) based his method on observable characteristics that are indirect indices of these parameters. These characteristics include slope height, slope inclination, degree of weathering, strength of induration, openness of fissures, spacing of fissures, vegetation, and moisture conditions. To derive criteria for rating slope-failure

susceptibility, these eight slope characteristics were organized into a decision tree. Additional criteria were established for pre-existing landslide deposits and engineered slopes. Thus, susceptibility was assigned to slopes based on the sequence of slope characteristics in the decision tree and was modified for the additional criteria. We follow this procedure to map bedrock-slope-failure hazards in the central Cache Valley, with modifications from Keefer (1993) noted below. Our sources for slope characteristics and additional criteria are listed in table 17. We implement the decision tree by first creating map overlays that correspond to the Keefer (1993) criteria (steps 1 through 11) and then combining the overlays in various combinations corresponding to the decision-tree branches (steps 12 through 22). Alternate techniques may be used with GIS software that lacks the ability to create a new map layer defined by the intersection of two or more input map layers. These techniques include the use of grid queries to determine which map cells satisfy certain criteria corresponding to the decision-tree branches and the use of cross-tabulation to record all combinations of input data for each map cell.

Table 17. *Data sources used in this study to characterize criteria for analyzing rock-slope-failure susceptibility.*

Criteria	Options	Data Source
Slope Height	>2,000 m	Topographic maps
	<2,000 m	
Slope Inclination	>25°	USGS DEM
	<25°	
Weathering	Intensely weathered	Geologic-map-unit descriptions, field observations
	Not intensely weathered	
Induration	Poorly indurated	Geologic-map-unit descriptions
	Not poorly indurated	
Open Fissures	Present	Field observations, aerial photographs
	Absent	
Fissure Spacing	Close	Geologic-map-unit descriptions
	Not close	
Vegetation	Present	Not used (may be obtained from NRCS or USGS digital map layers)
	Absent	
Moisture	Wet	Assume wet
	Dry	
Landslides	Yes	Geologic maps
	No	
Engineered Slopes	Yes	Field observations, geologic maps
	No	

Step 1: Map all pre-Quaternary geologic units. We consider all pre-Quaternary units to be bedrock and map their seismic slope stability in the following steps. All Quaternary units are considered soil and their seismic slope stability was mapped using procedures in previous sections of this report for mapping lateral-spread and translational-landslide hazards.

Step 2: Map slope inclination by mapping two slope units from the USGS DEM within areas

underlain by bedrock. One unit includes all areas with slopes less than 25 degrees, the other unit includes all areas with slopes greater than 25 degrees.

Step 3: Map weathering by mapping intensely weathered bedrock materials, identified by Keefer (1993) as typically consisting of heterogenous mixtures of cobbles, blocks, and boulders in a fine matrix, grading into residual soils at the ground surface. We found no extensive areas of intensely weathered materials in our study area.

Step 4: Map induration by mapping poorly indurated bedrock, identified by Keefer (1993) as rocks that typically crumble into small fragments when disturbed, cannot be excavated in intact blocks, and have unconfined compressive strengths less than 700 kPA. On a regional scale, we consider all Tertiary geologic units in our study area to be poorly indurated and all other bedrock units to be indurated to a greater degree.

Step 5: Map bedrock with open fissures. In the central Cache Valley, we observed in the field that almost all cliffs that have shed talus have some open fissures. We therefore constructed a photogeologic map of rock-fall source areas based on the distribution of cliffs and talus. These areas are assumed to contain open fissures. All other areas underlain by bedrock are assumed to contain no open fissures.

Step 6: Map bedrock with closely spaced fissures, defined by Keefer (1993) as a rock mass broken by at least two sets of fissures with average spacings of a few centimeters or less. In the central Cache Valley, two brecciated units of Precambrian to Cambrian age are mapped on the northern edge of the Smithfield quadrangle near Crow Mountain (Lowe and Galloway, 1993). We consider these two map units, an informally named quartzite and the Geertsen Canyon (?) Quartzite, to have close fissure spacing. All other bedrock units are considered to have spacing that is not close.

Step 7: Map moisture. Keefer (1993) determined if slope units were wet at the time of historical seismically induced landslides by noting if heavy rainfall had occurred in the few days preceding earthquakes, if water was observed seeping out of the slopes, or if slope materials were wet when examined in hand specimens. Because periods of slope moisture may be temporary and brief but may decrease rock-slope stability, we conservatively assume that all rock slopes in our study area will be wet when affected by earthquakes.

Step 8: Map slope height by mapping bedrock slopes where elevation differences between the lowest and highest parts of the slopes are more than 2,000 meters. Keefer (1993) noted that landslide concentrations were particularly great in areas where topographic relief exceeds this threshold. No slopes in our study area meet this criterion because the maximum relief is 1,122 meters, from the Bonneville shoreline to Big Baldy in the Bear River Range east of Millville (plate 3D).

Step 9: Map vegetated bedrock slopes from digital vegetation map layers available from the U.S. Natural Resources Conservation Service (NRCS) or USGS. Keefer (1993) observed that

slopes lacking vegetation produced higher concentrations of landslides than vegetated slopes in otherwise similar materials, but only for earthquakes with magnitudes less than or equal to 6.5. Because we do not specify an earthquake magnitude in our analysis of bedrock-slope-failure hazards, we do not map vegetated bedrock slopes.

Step 10: Map engineered slopes by mapping bedrock slopes engineered with reinforced retaining walls or other, well-anchored retaining structures. Keefer (1993) determined that such slopes have a low susceptibility to earthquake-induced failure, regardless of geologic setting. We found no extensive engineered slopes in our study area.

Step 11: Map pre-existing landslide deposits, which are susceptible to renewed failure during earthquakes.

Step 12: Determine the contribution of slope inclination (step 2) to the slope-failure hazard.

a. If slopes are greater than 25 degrees, proceed to step 13.
b. If slopes are less than 25 degrees, the slope-failure hazard is low unless modified by steps 19 through 22. Skip to step 19 to determine the final slope-failure hazard.

Step 13: Determine the contribution of weathering (step 3) to the slope-failure hazard.

a. If rocks are intensely weathered, the slope-failure hazard is extremely high unless modified by steps 19 through 22. Skip to step 19 to determine the final slope-failure hazard.
b. If rocks are not intensely weathered, proceed to step 14.

Step 14: Determine the contribution of induration (step 4) to the slope-failure hazard.

a. If rocks are poorly indurated, the slope-failure hazard is very high unless modified by steps 19 through 22. Skip to step 19 to determine the final slope-failure hazard.
b. If rocks are not poorly indurated, proceed to step 15.

Step 15: Determine the contribution of open fissures (step 5) to the slope-failure hazard.

a. If rocks have open fissures, proceed to step 16.
b. If rocks do not have open fissures, skip to step 17.

Step 16: Determine the contribution of fissure spacing (step 6) to the slope-failure hazard.

a. If fissures are closely spaced, the slope-failure hazard is high unless modified by steps 19 through 22. Skip to step 19 to determine the final slope-failure hazard.
b. If fissures are not closely spaced, skip to step 18.

Step 17: Determine the contribution of fissure spacing (step 6) to the slope-failure hazard.

a. If fissures are closely spaced, proceed to step 18.
b. If fissures are not closely spaced, the slope-failure hazard is moderate unless modified by steps 19 through 22. Skip to step 19 to determine the final slope-failure hazard.

At this point, Keefer (1993) designates the hazard as low rather than moderate. Because

of the progression of the hazard assessment from step 12 (slope inclination) through step 17 (fissure spacing), this results in a low hazard potential for some steep slopes (greater than 25 degrees). Generally, we do not recommend site-specific investigations to assess hazards in areas with a low hazard potential except for essential facilities and special- and high-occupancy buildings (table 6). However, because of our limited data on existing slopes, we believe that site-specific investigations for the slope-failure hazard should be conducted for all development types on steep slopes, and therefore map all steep slopes with at least a moderate hazard potential. We therefore assign a moderate hazard potential to the conditions that prevail at step 17b, unless modified by steps 19 through 22.

Step 18: Determine the contribution of moisture (step 7) to the slope-failure hazard.

a. If slopes are wet, the slope-failure hazard is high unless modified by steps 19 through 22. Proceed to step 19 to determine the final slope-failure hazard.
b. If slopes are dry, the slope-failure hazard is moderate unless modified by steps 19 through 22. Proceed to step 19 to determine the final slope-failure hazard.

Step 19: Determine the contribution of relief (step 8) to the slope-failure hazard.

a. If slope height is greater than 2,000 meters, increase the hazard rating by one level except for slope units rated low or extremely high; proceed to step 20.
b. If slope height is less than 2,000 meters, the hazard rating is unchanged; proceed to step 20.

Step 20: Determine the contribution of vegetation (step 9) to the slope-failure hazard.

a. If slopes are vegetated, decrease the hazard rating by one level if the hazard scenario assumes an earthquake with a magnitude less than or equal to 6.5.
b. If slopes are not vegetated, the hazard rating is unchanged; proceed to step 21.

Step 21: Determine the contribution of engineered slopes (step 10) to the slope-failure hazard.

a. If engineered slopes are present, the hazard rating is low regardless of previous analysis.
b. If engineered slopes are not present, the hazard rating is unchanged; proceed to step 22.

Step 22: Determine the contribution of landslides (step 11) to the slope-failure hazard.

a. If pre-existing landslide deposits are present, the hazard rating is high regardless of previous analysis.
b. If pre-existing landslide deposits are not present, the hazard rating is unchanged.

Results

By analyzing earthquake-induced slope-failure hazards of the central Cache Valley using a three-tiered approach, we identify the relative hazard potential of the dominant process that affects slopes in each specific area. Slope inclination and the degree of consolidation of earth materials are the primary criteria used to determine the appropriate process for analysis. Similar geotechnical properties and ground-water depth may result in differing hazard potentials depending upon the

selected analytical technique. For each specific technique, the choice of earthquake parameters may affect hazard potential, although the relative hazard should remain consistent.

We map a very high potential for earthquake-induced slope failure on limited parts of the Bear River Range front east of Smithfield (plate 3B) and Wellsville Mountains front west of Wellsville (plate 3C). These slopes are susceptible to bedrock-slope failure because they are steep (with an inclination greater than 25 degrees) and underlain by poorly indurated deposits mapped as the Tertiary Salt Lake Formation (McCalpin, 1989). Upper Pleistocene to Holocene landslides are common within similar deposits throughout the valley (McCalpin, 1989; Solomon, 1999).

We map a high potential for earthquake-induced slope failure in scattered areas throughout the central Cache Valley. The potential for bedrock-slope failures is locally high in mountain slopes underlain by Paleozoic rocks with open fissures. These rocks are most common in Logan, Dry, and Providence Canyons east and southeast of Logan and in steep, resistant cliffs in the Bear River Range east of Hyrum (plate 3D). The potential for lateral-spread failures is locally high in Holocene alluvium and in latest Pleistocene deposits of sand and silt of the Provo phase of Lake Bonneville. The most extensive area of high lateral-spread potential is east of Cutler Reservoir, where about 15 square kilometers are underlain by granular alluvium and alluvial-levee deposits of the Bear River saturated by shallow ground water (plate 3A). Scattered areas of high lateral-spread potential associated with Provo-phase sand and silt result from their location in areas of shallow ground water on slopes approaching the maximum slope inclination analyzed for lateral-spread potential. All landslides within the central Cache Valley are also mapped with a high potential for earthquake-induced slope failure. Solomon (1999) postulated liquefaction inducement for one of these landslides, a complex of slumps and flows of Lake Bonneville sand beneath Little Bear River alluvial-terrace deposits east of Wellsville formed after Holocene incision by the river to its present level (plate 3C). We map adjacent Lake Bonneville sand and silt deposits with a high potential for lateral-spread failures, supporting a liquefaction origin for the landslide and indicating a continuing threat in the area.

We map a moderate potential for earthquake-induced slope failure on most mountain slopes and on a significant part of the valley floor. The potential for bedrock-slope failures is moderate on most mountain slopes underlain by well-indurated Paleozoic rocks because of the high slope inclination (plates 3B, 3C, and 3D). The potential for lateral-spread failures is moderate in most flood plains of the Bear, Little Bear, and Logan Rivers (plates 3A, 3C, and 3D), on alluvial fans west of Smithfield (plate 3B), and on the upper part of gentle slopes near Little Mountain, Cache Butte, and the Wellsville Mountains on the west side of the valley (plate 3A and 3C). Deposits with a moderate potential for lateral-spread failures are similar to those with a high potential, but have slightly lower slope inclinations.

We map a low potential for earthquake-induced slope failure on most mountain slopes with inclinations less than 25 degrees and on much of the valley floor. A low potential for bedrock-slope failures is most common east of Smithfield (plate 3B) where most of the Bear River Range front is underlain by deposits mapped as the Tertiary Salt Lake Formation. Because these rocks are soft and easily eroded, they are widespread on slopes with an inclination less than 25 degrees. A low

potential for lateral-spread failures is associated with deposits of Lake Bonneville silt and clay, which generally lack thick layers of granular material that are susceptible to liquefaction and commonly underlie the flat valley floor (plates 3A, 3B, 3C, and 3D).

We map a very low potential for earthquake-induced slope failure on the piedmont slopes of the central Cache Valley and on the flat valley bottom. A very low potential for lateral-spread failures is most common on the east side of the valley where ground water is too deep to saturate susceptible soil (plates 3B and 3D) and in the south part of the study area where both susceptibility and slope are very low (plates 3C and 3D). A very low potential for translational landslides is mapped on the perimeter of the valley floor where slopes are too gentle to pose a significant hazard (plates 3A, 3B, 3C, and 3D).

Our maps provide a regional assessment of earthquake-induced slope-failure hazards in the central Cache Valley, but care should be used for proper application of the mapping techniques and data. Each of our analytical methods incorporate assumptions that are necessary for practical application of the techniques to regional studies.

Ground displacements calculated for lateral spreading depend upon earthquake magnitude, distance to the earthquake source, texture of liquefiable sediments, and ground-water depth. For this map, we assume an earthquake of magnitude 6.5 occurs at a constant distance of 5 kilometers from each map point, but these conditions may vary. To adjust displacements for a different earthquake magnitude and distance, use the appropriate multiplication factor from table 18. We also assume that liquefiable sediments consist of silty sand with a fines content of 30 percent and a mean grain size of 0.2 millimeters. Because textures in natural settings are both vertically and horizontally variable and we have little data on sediment textures, site-specific geotechnical investigations are required to develop accurate estimates of texture. The effects of differing textures can be determined using the appropriate multiplication factor from table 19 to adjust displacements calculated for this study. Multiplication factors in both tables are calculated using the equation of Youd and others (1999) for ground-slope conditions. Site-specific investigations are needed for accurate measurement of ground-water depth.

Although we estimate liquefaction-induced ground displacement caused by lateral spreading, liquefaction-induced ground displacement may also be caused by flow failure, ground oscillation, and ground settlement. We do not estimate potential ground displacement that may result from these mechanisms. Except for some locally steep river banks, ground slopes in liquefiable areas of the central Cache Valley are too gentle to be susceptible to flow failure. No widely accepted techniques for estimating transient lateral displacements generated from liquefaction-induced ground oscillation exist, but Mabey and others (1993) suggest using the greater of a few tenths of a meter or the predicted displacement for lateral spread as a preliminary estimate. Techniques for estimating settlements in granular soils during earthquakes (Tokimatsu and Seed, 1987; Ishihara and Yoshimine, 1992) were developed for clean sands and have not been fully verified for silty sands and sandy silts that commonly underlie the central Cache Valley. Mabey and others (1993) estimate that a 10-meter thick liquefiable layer of silty sand might be expected to generate settlements on the order of 0.1 to 0.5 meters during strong earthquakes. Smaller amounts of non-liquefaction-induced

settlement could be generated in loose granular sediments above the water table.

Table 18. *Multiplication factors to adjust lateral ground displacements for different earthquake magnitudes and distances to seismic source (using the equation of Youd and others [1999]). The default condition is shaded.*

Earthquake Magnitude[1]	0.25	1	5	10	20	30	40	50	60	70	80	90	100
6.0	4.7	1.6	0.2	0.1	0	0	0	0	0	0	0	0	0
6.5	8.9	4.9	1.0	0.1	0	0	0	0	0	0	0	0	0
7.0	n.a.	10.	3.7	1.7	0.6	0.3	0.1	0.1	0.1	0	0	0	0
7.5	n.a.	n.a.	9.6	5.6	2.4	1.2	0.7	0.4	0.3	0.2	0.1	0.1	0.1
Distance to Seismic Source (km)													

[1] Lateral-spread displacement appears to decrease markedly for earthquakes with magnitudes less than 6 (Bartlett and Youd, 1992).
n.a.—not applicable. Predicted displacements for large earthquakes near seismic sources are larger than normally expected and actual displacements are not documented by adequate data; extrapolation of multiplication factors to these distances may yield unreliable results (Bartlett and Youd, 1992).

Table 19. *Multiplication factors to adjust lateral ground displacements for different textures of liquefiable sediments (modified from Mabey and others [1993] using the equation of Youd and others [1999]). The default condition is shaded.*

Unified Soil Classification	Description	Fines Content (%)	Mean Grain Size (mm)	Factor
SP or SW	Fine Sand	<5	<0.4	2.5
	Medium Sand		0.4-0.7	2.0
	Coarse Sand		>0.7	1.5
SP-SM or SW-SM	Fine Sand with Silt	5-12	<0.4	2.5
	Medium Sand with Silt		0.4-0.7	2.0
	Coarse Sand with Silt		>0.7	1.5
SM	Silty Fine Sand	12-30	<0.4	2.0
	Silty Medium Sand		0.4-0.7	1.5
	Silty Coarse Sand		>0.7	1.0
	Very Silty Sand	30-50	<0.4	1.0
ML	Sandy Silt	50-70	<0.08	0.4

Ground displacements calculated for translational landsliding depend upon earthquake

magnitude, peak ground accelerations, soil properties, and ground-water depth. For this map we assume an earthquake of magnitude 6.5 and a peak ground acceleration of 0.2 g, but larger earthquakes and ground accelerations are possible. We also assume representative values for shear strength and dry density of slope materials within each surficial geologic unit, and infer the proportion of slope materials that are saturated. Site-specific investigations are required to determine accurate soil properties and ground-water depth. Our recommendations for the need to conduct site-specific investigations are shown in table 6.

Our slope-failure-hazard maps indicate only the source zones of landslides (the parts of slopes that may fail). This map does not show how far downslope the failed material may travel before stopping. Proposed development in areas downslope of landslide source zones should consider this in site-specific investigations. Our maps are also limited by the size of potential slope failures that can be considered in a regional mapping study. Small failures caused by locally steep terrain not readily apparent on the slope map, or pockets of colluvium on a steep rock slope, cannot be identified at this scale. The slope-failure ratings do not consider hazards caused by cuts, fills, or other alterations to the natural terrain.

SUMMARY AND CONCLUSIONS

In this report, we define procedures to map seismic hazards in the central Cache Valley, primarily using existing data. This area, near the populous Wasatch Front region of northern Utah, is largely rural but contains several rapidly developing cities and towns. Because of its rural nature, subsurface geotechnical data are clustered in population centers and are sparse elsewhere. Therefore, we rely upon surrogate subsurface geotechnical data derived from abundant water wells. Our procedures are suitable for seismic-hazard assessment elsewhere along the Wasatch Front, and in other rural areas underlain by thick deposits of unconsolidated material where similar amounts of geotechnical and water-well data exist. However, the use of water-well data is not a suitable substitute for direct measurement of geotechnical properties where geotechnical data exist or may be conveniently obtained. The use of a regional hazard assessment, whether derived from water-well or geotechnical data, is never a suitable subsititute for a site-specific geotechnical investigation.

We mapped amplified-ground-shaking, surface-fault-rupture, liquefaction, and seismic-slope-instability hazards in the central Cache Valley. Although the potential for each hazard is largely independent of the others, certain areas are at greater risk from combinations of seismic hazards. The greatest hazard potential is generally in the center of the valley. Here, relatively thick Lake Bonneville clay is locally overlain by more recent saturated, sandy alluvium. The clay contributes to greater amplification of earthquake ground motions along the valley bottom from The Barrens in the north, through Cutler Reservoir, to the Little Bear River in the south. The alluvium contributes to a higher potential for liquefaction in the Bear, Little Bear, and Logan River flood plains and liquefaction-induced lateral spreading in the Bear River flood plain and adjacent alluvial levees. Much of the remainder of the valley floor and the mountains bordering the valley are subject to low to moderate seismic hazards, although higher hazards exist locally. Steep mountain slopes are predominantly subject to a moderate hazard from earthquake-induced slope failure.

Most development in the central Cache Valley is along the valley margins on piedmont slopes, and these areas will be the primary focus of development pressures in the immediate future. These developed areas have generally lower seismic-hazard potentials, particularly along the east side of the valley. The communities of Smithfield, Hyde Park, North Logan, Logan, Providence, Millville, and Hyrum all lie, for the most part, in very-low- to low-hazard areas along the east side of the valley. Here, coarser-grained soil results in lower amplification of earthquake ground motions, ground water is too deep for a significant liquefaction hazard, and slopes are too gentle for a significant slope-failure hazard. The active East Cache fault zone lies at the base of the Bear River Range near all of these communities, but the associated surface-fault-rupture hazard is limited to areas directly adjacent to the fault. The communities of Newton, Mendon, and Wellsville all lie, for the most part, in low- to moderate-hazard areas along the west side of the valley. These communities are subject to similar amplification of earthquake ground motions as on the east side of the valley, but hazards from liquefaction and lateral spreading are greater. The West Cache fault zone lies to the west of these communities and does not pose an immediate threat of surface-fault rupture. However, as development proceeds into currently undeveloped areas, extending from both valley margins into the center of the valley and into the mountains, exposure to seismic hazards will increase.

Our maps are intended primarily for regional purposes. The maps are appropriate to use as a tool for local-government officials in guiding safe and responsible development through incorporation into a land-use plan or zoning ordinance. The maps may also be used to prepare earthquake planning scenarios and loss estimates, require site-specific geotechnical investigations, or increase earthquake awareness, education, and training. Geologists and engineers may use technical information on the maps to devise plans for addressing the hazards. However, the maps are not intended for use at scales other than the published scale. Hazard boundaries are based on geologic criteria and limited subsurface data and are therefore approximate and subject to change with additional data. The hazard at any particular site may actually be higher or lower than shown because of geological variations within map boundaries, gradational and approximate map boundaries, and the regional scale of the maps.

ACKNOWLEDGEMENTS

This study was completed through a cooperative project funded by the Utah Geological Survey (UGS), USGS NEHRP, Bear River Association of Governments, and Cache County. We thank Jay Aguilar, Bear River Association of Governments, and Thad Erickson, Lynn Lemon, and Mark Teusher, Cache County, for their guidance and help in funding this project. We also thank Greg McDonald, UGS, for his assistance compiling the water-well database; David Simon, Simon-Bymaster, Inc., for contributing geotechnical-borehole logs; Leslie Heppler, Utah Department of Transportation, for letting us search files for geotechnical-borehole logs; the Utah Division of Water Rights for letting us search files for water-well logs; and Dr. Loren Anderson, University of Utah, for contributing geotechnical data from the liquefaction study of the northern Wasatch Front that he coauthored. Discussions with Gary Christenson, UGS, were helpful throughout this project. The report was improved by thoughtful reviews by both Gary Christenson and Dr. Jeffrey Keaton, AMEC

Earth & Environmental, Inc, who reviewed the section of the report on liquefaction.

REFERENCES

Anderson, L.R., Keaton, J.R., Aubry, Kevin, and Ellis, S.J., 1982, Liquefaction potential map for Davis County, Utah: Logan, Utah State University Department of Civil and Environmental Engineering and Dames and Moore unpublished Final Technical Report for the U.S. Geological Survey, 50 p.; published as Utah Geological Survey Contract Report 94-7, 1994.

Anderson, L.R., Keaton, J.R., and Bay, J.A., 1990a, Liquefaction potential map for the northern Wasatch Front, Utah: Logan, Utah State University Department of Civil and Environmental Engineering unpublished Final Technical Report for the U.S. Geological Survey, 150 p.; published as Utah Geological Survey Contract Report 94-6, 1994.

Anderson, L.R., Keaton, J.R., and Bischoff, J.E., 1986a, Liquefaction potential map for Utah County, Utah: Logan, Utah State University Department of Civil and Environmental Engineering and Dames and Moore unpublished Final Technical Report for the U.S. Geological Survey, 46 p.; published as Utah Geological Survey Contract Report 94-8, 1994.

Anderson, L.R., Keaton, J.R., and Rice, J.D., 1990b, Liquefaction potential map for central Utah: Logan, Utah State University Department of Civil and Environmental Engineering unpublished Final Technical Report for the U.S. Geological Survey, 134 p.; published as Utah Geological Survey Contract Report 94-10, 1994.

Anderson, L.R., Keaton, J.R., Spitzley, J.E., and Allen, A.C., 1986b, Liquefaction potential map for Salt Lake County, Utah: Logan, Utah State University Department of Civil and Environmental Engineering and Dames and Moore unpublished Final Technical Report for the U.S. Geological Survey, 48 p.; published as Utah Geological Survey Contract Report 94-9, 1994.

Arias, A., 1970, A measure of earthquake intensity, *in* Hansen, R.J., editor, Seismic design for nuclear power plants: Cambridge, Massachusetts Institute of Technology Press, p. 438-483.

Ashland, F.X., and Rollins, Kyle, 1999, Seismic zonation using geotechnical site-response mapping, Salt Lake Valley, Utah: Utah Geological Survey and Brigham Young University Department of Civil and Environmental Engineering Final Technical Report for the U.S. Geological Survey, 33 p.

Bartlett, S.F., and Youd, T.L., 1992, Empirical analysis of horizontal ground displacement generated by liquefaction-induced lateral spreads: National Center for Earthquake Engineering Research Technical Report NCEER-92-0021, 114 p.

Bjorklund, L.J., and McGreevy, L.J., 1971, Ground-water resources of Cache Valley, Utah and

Idaho: Utah Department of Natural Resources Technical Publication 36, 72 p.

Black, B.D., Giraud, R.E., and Mayes, B.H., 2000, Paleoseismic investigation of the Clarkston, Junction Hills, and Wellsville faults, West Cache fault zone, Cache County, Utah: Utah Geological Survey Special Study 98, 23 p.

Building Seismic Safety Council, 1997, NEHRP recommended provisions for seismic regulations for new buildings and other structures: Washington, D.C., Federal Emergency Management Agency Publication 302, Part 1 – Provisions, 337 p.

California Division of Mines and Geology, 1997, Guidelines for evaluating and mitigating seismic hazards in California: California Department of Conservation, Division of Mines and Geology Special Publication 117, 74 p.

Chang, W.L., and Smith, R.B., 1998, Potential for tectonically induced tilting and flooding by the Great Salt Lake, Utah, from large earthquakes on the Wasatch fault, *in* Lund, W.R., editor, Proceedings volume—Basin and Range Province seismic-hazards summit: Utah Geological Survey Miscellaneous Publication 98-2, p. 128-138.

Christenson, G.E., 1993, Wasatch Front County Hazards Geologist Program, *in* Gori, P.L., editor, Applications of research from the U.S. Geological Survey program, Assessment of Regional Earthquake Hazards and Risk Along the Wasatch Front, Utah: U.S. Geological Survey Professional Paper 1519, p. 114-120.

Dobry, R., Idriss, I.M., and Ng, E., 1978, Duration characteristics of horizontal components of strong-motion earthquake records: Bulletin of the Seismological Society of America, v. 68, no. 5, p. 1487-1520.

Environmental Systems Research Institute, Inc., 1999, ArcView GIS v3.2: Redlands, California, Environmental Systems Research Institute, Inc.

—2000, ArcView Spatial Analyst v2.0a: Redlands, California, Environmental Systems Research Institute, Inc.

Evans, J.P., McCalpin, J.P., and Holmes, D.C., 1996, Geologic map of the Logan quadrangle, Cache County, Utah: Utah Geological Survey Miscellaneous Publication 96-1, scale 1:24,000.

Frankel, Arthur, Mueller, Charles, Barnhard, Theodore, Perkins, David, Leyendecker, E.V., Dickman, Nancy, Hanson, Stanley, and Hopper, Margaret, 1996, National seismic-hazard maps—documentation June 1996: U.S. Geological Survey Open-File Report 96-532, 110 p.

Green, K.R., 1977, A study of geologic hazards and geotechnical input for selected critical facilities—Cache Valley, Utah: Logan, Utah State University, unpublished M.S. thesis, 131

Hill, R.J., 1979, A liquefaction potential map for Cache Valley, Utah: Logan, Utah State University, unpublished M.S. thesis, 96 p.

Hofmeister, R.J., 1999a, Earthquake-induced slope instability—A relative hazard map for the Salem Hills, Oregon: Oregon Department of Geology and Mineral Industries Special Paper 30.

—1999b, Earthquake-induced slope instability—A relative hazard map for the vicinity of the Salem Hills, Oregon: Oregon Geology, v. 61, no. 3, p. 55-63.

International Code Council, 1997, International Building Code 2000—First Draft: Birmingham, Alabama, 35 chapters.

International Conference of Building Officials, 1997, Uniform Building Code; Volume 2: Whittier, California, 492 p.

Ishihara, K., 1985, Stability of natural soil deposits during earthquakes: Proceedings of the 11th International Conference of Soil Mechanics and Foundation Engineering, San Francisco, v. 1, p. 321-376.

Ishihara, K., and Yoshimine, M., 1992, Evaluation of settlements in sand deposits following liquefaction during earthquakes: Soils and Foundations, v. 32, no. 1, p. 173-188.

Jibson, R.W., 1993, Predicting earthquake-induced landslide displacements using Newmark's sliding block analysis: Transportation Research Record, no. 1411, p. 9-17.

Jibson, R.W., Harp, E.L., and Michael, J.A., 1998, A method for producing digital probabilistic seismic landslide hazard maps—an example from the Los Angeles, California, area: U.S. Geological Survey Open-File Report 98-113, 17 p.

Keaton, J.R., 1986, Potential consequences of tectonic deformation along the Wasatch fault: Logan, Utah State University Department of Civil and Environmental Engineering, Final Technical Report for the U.S. Geological Survey.

Keaton, J.R., and Anderson, L.R., 1995, Mapping liquefaction hazards in the Wasatch Front region—opportunities and limitations, *in* Lund, W.R., editor, Environmental and engineering geology of the Wasatch Front region: Utah Geological Association Publication 24, p. 453-468.

Keaton, J.R., Anderson, L.R., Topham, D.E., and Rathbun, D.J., 1987, Earthquake-induced landslide potential in and development of a seismic slope stability map of the urban corridor of Davis and Salt Lake Counties, Utah: Logan, Utah State University Department of Civil and Environmental Engineering and Dames and Moore, Final Technical Report for the U.S. Geological Survey, 47 p.

Keefer, D.K., 1993, The susceptibility of rock slopes to earthquake-induced failure: Bulletin of the Association of Engineering Geologists, v. 30, no. 3, p. 353-361.

Keefer, D.K., and Wang, Yumei, 1997, A method for predicting slope instability for earthquake hazard maps—Preliminary report, *in* Wang, Yumei, and Neuendorf, K.K.E., editors, Earthquakes—Converging at Cascadia: Oregon Department of Geology and Mineral Industries Special Paper 28 and Association of Engineering Geologists Special Publication 10, p, 39-52.

Keefer, D.K., Wieczorek, G.F., Harp, E.L., and Tuel, D.H., 1979, Preliminary assessment of seismically induced landslide susceptibility, *in* Brabb, E.E., editor, Progress on seismic zonation in the San Francisco Bay region: U.S. Geological Survey Circular 807, p. 49-60.

Keefer, D.K., and Wilson, R.C., 1989, Predicting earthquake-induced landslides, with emphasis on arid and semi-arid environments, *in* Sadler, P.M., and Morton, D.M., editors, Landslides in a semi-arid environment: Riverside, California, Inland Geological Society, vol. 2, p. 118-149.

King, K.W., Williams, R.A., and Carver, D.L., 1987, Relative ground response in Salt Lake City and areas of Springville-Spanish Fork, Utah, *in* Gori, P.L., and Hays, W.W., editors, Assessment of regional earthquake hazards and risk along the Wasatch Front, Utah: U.S. Geological Survey Open-File Report 87-585, v. 2, p. N1-N48.

Lander, J.F., and Cloud, W.K., 1964, United States earthquakes, 1962: Washington, D.C., U.S. Department of Commerce, Coast and Geodetic Survey, United States Earthquake Series, p. 112-113.

Lowe, Mike, and Galloway, C.L., 1993, Provisional geologic map of the Smithfield quadrangle, Cache County, Utah: Utah Geological Survey Map 143, scale 1:24,000.

Mabey, M.A., Madin, I.P., Youd, T.L., and Jones, C.F., 1993, Earthquake hazard maps of the Portland quadrangle, Multnomah and Washington Counties, Oregon, and Clark County, Washington: Oregon Department of Mineral Industries Geologic Map Series GMS-79, scale 1:24,000.

McCalpin, James, 1989, Surficial geologic map of the East Cache fault zone, Cache County, Utah: U.S. Geological Survey Miscellaneous Field Studies Map MF-2107, scale 1:50,000.

—1994, Neotectonic deformation along the East Cache fault zone, Cache County, Utah: Utah Geological Survey Special Study 83, 37 p.

—1996, Using GIS to predict zones of earthquake-induced landsliding in Seattle, Washington: Geological Society of America, Abstracts with Programs, v. 28, no. 7, p. 526.

McCalpin, J.P., and Nishenko, S.P., 1996, Holocene paleoseismicity, temporal clustering, and probabilities of future large (M > 7) earthquakes on the Wasatch fault zone, Utah: Journal of Geophysical Research, v. 101, no. B3, p. 6,233-6,253.

Monahan, P.A., Levson, V.M., McQuarrie, E.J., Bean, S.M., Henderson, Paul, and Sy, Alex, 2000, Relative earthquake hazard map of greater Victoria, showing areas susceptible to amplification of ground motion, liquefaction, and earthquake-induced slope instability: British Columbia Ministry of Energy and Mines, Geological Survey Branch Geoscience Map 2000-1, scale 1:25,000.

Newmark, N.M., 1965, Effects of earthquakes on dams and embankments: Geotechnique, v. 15, no. 2, p. 139-160.

Obermeier, S.F., 1996, Using liquefaction-induced features for paleoseismic analyis, *in* McCalpin, J.P., editor, Paleoseismology, New York, Academic Press, p. 331-396.

Personius, S.F., 1991, Paleoseismic analysis of the Wasatch fault zone at the Brigham City trench site, Brigham City, Utah and Pole Patch trench site, Pleasant View, Utah: Utah Geological and Mineral Survey Special Study 76, 39 p.

Rial, J.A., Saltzman, N.G., and Ling, H., 1992, Earthquake-induced resonance in sedimentary basins: American Scientist, v. 80, p. 566-578.

Schnabel, P.B., Lysmer, J., and Seed, H.B., 1972, SHAKE—A computer program for earthquake analysis of horizontally layered sites: Berkeley, University of California, Earthquake Engineering Research Center Report EERC 72-12, 88 p.

Schuster, R.L., and Chleborad, A.F., 1990, Ground failure associated with the Puget Sound region earthquakes of April 13, 1949 and April 29, 1965: U.S. Geological Survey Open-File Report 90-687, 129 p.

Scott, W.E., McCoy, W.D., Shroba, R.R., and Rubin, M., 1983, Reinterpretation of the exposed record of the last two cycles of Lake Bonneville, western United States: Quaternary Research, v. 20, p. 261-285.

Seed, H.B., 1979, Soil liquefaction and cyclic mobility evaluation for level ground during earthquakes: Journal of the Geotechnical Engineering Division, American Society of Civil Engineers, v. 102, p. 201-255.

Seed, H.B., and Idriss, I.M., 1982, Ground motions and soil liquefaction during earthquakes: Berkeley, California, Earthquake Engineering Research Institute Monograph Series.

Seed, H.B., Idriss, I.M., and Arango, I., 1983, Evaluation of liquefaction potential using field performance data: Journal of the Geotechnical Engineering Division, American Society of

Civil Engineers, v. 109, no. 3, p. 458-482.

Seed, H.B., Tokimatsu, K., Harder, L.F., and Chung, R., 1985, Influence of SPT procedures on soil liquefaction resistance evaluations: Journal of the Geotechnical Engineering Division, American Society of Civil Engineers, v. 111, no. 12, p. 1425-1445.

Shannon & Wilson, Inc., and Agbabian Associates, 1980, Geotechnical and strong motion earthquake data from U.S. accelerograph stations: U.S. Nuclear Regulatory Commission, NUREG/CR-0985, v. 3, p. 63-113.

Simon-Bymaster, Inc., 1998, Geotechnical engineering study, North Logan 3rd, 7th, & Green Canyon Stake, 400 East 1800 North, North Logan, Utah: Bountiful, Utah, unpublished consultant's report, 23 p.

—1999, Liquefaction evaluation, North Logan 3rd, 7th, & Green Canyon Stake, 400 East 1800 North, North Logan, Utah: Bountiful, Utah, unpublished consultant's report, 22 p.

Solomon, B.J., 1999, Surficial geologic map of the West Cache fault zone and nearby faults, Box Elder and Cache Counties, Utah: Utah Geological Survey Map 172, scale 1:50,000.

Somerville, P.G., 1998, Emerging art–earthquake ground motion, *in* Dakoulas, P., Yegian, M., and Holtz, R.D., editors, Geotechnical earthquake engineering and soil dynamics III: American Society of Civil Engineers, Geotechnical Special Publication 75, p. 1-38.

Somerville, P.G., Smith, N.F., Graves, R.W., and Abrahamson, N.A., 1997, Modification of empirical strong ground motion attenuation relations to include the amplitude and duration effects of rupture directivity: Seismological Research Letters, v. 68, no. 1, p. 199-222.

Southern California Earthquake Center, 1999, Recommended procedures for implementation of DMG Special Publication 117—Guidelines for analyzing and mitigating liquefaction in California: Los Angeles, University of Southern California, Southern California Earthquake Center, 63 p.

Tokimatsu, K., and Seed, H.B., 1987, Evaluation of settlements in sands due to earthquake shaking: Journal of Geotechnical Engineering, v. 113, no. 8, p. 861-878.

Wieczorek, G.F., Wilson, R.C., and Harp, E.L., 1985, Map showing slope stability during earthquakes of San Mateo County, California: U.S. Geological Survey Miscellaneous Geologic Investigations Map I-1257E, scale 1:62,500.

Williams, R.A., King, K.W., and Tinsley, J.C., 1993, Site response estimates in Salt Lake Valley, Utah from borehole seismic velocities: Bulletin of the Seismological Society of America, v. 83, no. 3, p. 862-889.

Wilson, R.C., and Keefer, D.K., 1985, Predicting areal limits of earthquake-induced landsliding, *in* Ziony, J.I., editor, Evaluating Earthquakes in the Los Angeles Region: U.S. Geological Survey Professional Paper 1360, p. 317-345.

Wong, I.G., and Silva, W.J., 1993, Site-specific strong ground motion estimates for Salt Lake Valley, Utah: Utah Geological Survey Miscellaneous Publication 93-9, 34 p.

Youd, T.L, 1980, Ground failure displacement and earthquake damage to buildings: American Society of Civil Engineers conference on civil engineering and nuclear power, 2d, Knoxville, Tennessee, 1980, v. 2, p. 7-6-2 – 7-6-26.

—1991, Mapping of earthquake-induced liquefaction for seismic zonation: International Conference on Seismic Zonation, 4th, August 1991, Stanford, California, Proceedings, p. 111-147.

Youd, T.L, Hansen, C.M., and Bartlett, S.F., 1999, Revised MLR equations for predicting lateral spread displacement, *in* Proceedings, 7th U.S.-Japan Workshop on Earthquake Resistant Design of Lifeline Facilities and Countermeasures Against Liquefaction, Seattle, Washington: Multidisciplinary Center for Earthquake Engineering Research Technical Report MCEER-99-0019, p. 99-114.

Youd, T.L., and Perkins, D.M., 1978, Mapping liquefaction-induced ground failure potential: Journal of the Geotechnical Engineering Division, American Society of Civil Engineers, v. 104, p. 433-446.